This is a non peer-reviewed preprint submitted to EarthArXiv

Manuscript submitted to PNAS

Modest, not extreme, northern high latitude amplification over the Mid to Late Miocene shown by coccolith clumped isotopes

Luz María Mejía[a,b*], Stefano M. Bernasconi[a], Alvaro Fernandez[c], Hongrui Zhang[a,d], José Guitián[a,e], Madalina Jaggi[a], Victoria E. Taylor[f], Alberto Perez-Huerta[g], Heather Stoll[a]

[a] Geological Institute, ETH Zürich, Sonneggstrasse 5, ETH, 8092, Zürich, Switzerland
[b] Now at MARUM, University of Bremen, 28359 Bremen, Germany
[c] Instituto Andaluz de Ciencias de la Tierra, Av. de las Palmeras 4, 18100 Armilla, Granada, Spain
[d] Now at Tongji University, Siping Road 1239, Shanghai, China
[e] Now at Centro de Investigación Mariña, Universidade de Vigo, GEOMA, Vigo, 36310, Spain
[f] Department of Earth Science, University of Bergen, Allegaten 41, 5007, Bergen, Norway
[g] Department of Geological Sciences, University of Alabama, Tuscaloosa, AL 35487, USA

* Corresponding author: lmejia@marum.de

Author contributions
L.M.M and H.Z developed the separation method; A.F applied the diagenesis model; L.M.M separated and cleaned the coccoliths, estimated authigenic carbonate; L.M.M and M.J measured clumped isotopes under the direction of S.B; L.M.M and M.J prepared and measured samples for trace element analysis. L.M.M and A.P.H took the SEM pictures; H.Z. evaluated coccolith assemblages. L.M.M purified alkenones and L.M.M and J.G. measured alkenones. L.M.M wrote the paper with contributions from A.F, S.B, H.S, H.Z and V.T.

Competing interests
There are no competing interests.

Classification
Physical Sciences, Earth Sciences

Keywords
Coccolithophores, Clumped Isotopes, High Latitude Amplification, Miocene

This pdf includes
Main Text
Figures 1 to 5

Abstract

The ongoing global warming is characterized by a high latitude amplification effect, with Northern Hemisphere air temperatures increasing significantly faster than the global average. Widely-used paleotemperature proxies suggest that during past warm climate states, there was extreme high-latitude and polar amplified warming, along with flat latitudinal sea surface temperature (SST) gradients. Because these features remain difficult to simulate in climate models for periods like the Miocene, not only model construction, but also absolute values of proxy temperature estimates should be continuously revised. Clumped isotope thermometry is a tool that has the potential to bypass some of the limitations of other proxies, such as reliance on assumptions of past seawater chemistry, and other unknown mechanisms influencing their response to temperature changes. Here we provide the first downcore reconstruction of calcification temperatures from coccolith clumped isotopes (Δ_{47}) at northern high latitudes. This record shares trends with alkenone SSTs from the same samples estimated via widely-used calibrations, but suggest an on average ~9 °C colder North Atlantic over the last 16 million years (My). Coccolith Δ_{47} calcification temperatures agree better than alkenone-derived records with model simulations for the Mid and Late Miocene. If confirmed by additional records, a modest, rather than an extreme northern high latitude warmth, would entail paradigm-changing implications in our understanding of high latitude thermal response to anthropogenic CO_2, while implying a need for revision of the present interpretations of currently considered well-validated temperature proxies like alkenone unsaturation ratios.

Significance statement

Accurate predictions of future climate response to CO_2 depend on the ability of climate models to simulate past warmer climate states. However, one of the major paleoclimate conundrums is accurately simulating the extreme warmth seen at high latitudes during analog warm climates, like the Miocene. Our North Atlantic coccolith Δ_{47} temperature record is the first to agree well with Miocene modeling studies, suggesting a ~9 °C colder North Atlantic, and challenging the extreme high latitude amplification paradigm suggested by other proxies. This record highlights the need to reevaluate the ability of all proxies to achieve not only reliable trends, but also

absolute temperature values, while providing a more optimistic perspective of future high latitude climate response to CO_2 emissions.

Introduction

Temperature indicators such as foraminiferal $\delta^{18}O$ and Mg/Ca, archaeal tetraether index (TEX_{86}) and alkenone unsaturation index (U^{k}_{37}) generally show a consistent global cooling trend over the Cenozoic (e.g. refs. (1–3)). Such estimates have been used to test whether climate models used to predict future climate, can accurately simulate earth's climate response under high pCO_2, and other boundary conditions which differ from those of the observational period used to tune models. To date, the largest model-data discrepancies occur in the simulation of high latitude warmth, especially for the Miocene (~5.33-23.03 million years ago, Ma), because proxy data imply strong high latitude amplification and flattening of the latitudinal thermal gradient at warmer climate states (e.g. refs. (4, 5)). It is therefore unclear whether climate models are missing key physical processes, or if validity of reconstructed absolute temperature estimates and/or interpretation of well-established proxies needs to be re-examined, both of which can hamper accurate predictions of future climate. From all potential past analogs to future climate conditions, the Miocene is perhaps currently the most important, since we have already surpassed the CO_2 atmospheric concentrations (pCO_2) of the younger Pliocene (~2.58-5.33 Ma), and the modern continental configuration is significantly different to that of the older Eocene (~33.9-55.8 Ma). On the other hand, estimated Miocene pCO_2 and climate states correspond to middle, more realistic, future emission scenarios (RCP 4.5-6.0) (5). Therefore, an improved understanding of the thermal response of high latitudes to CO_2 forcing during the Miocene is necessary.

Clumped isotope (Δ_{47}) thermometry is a technique that estimates calcification temperatures based on the excess abundance of ^{13}C-^{18}O bonds, which are more stable at lower temperatures, compared to their abundance if the rare isotopes ^{13}C and ^{18}O were stochastically distributed among all isotopologues (6). The application of Δ_{47} to reconstruct temperatures has the advantage of being independent of seawater chemistry, in contrast to foraminiferal Mg/Ca and $\delta^{18}O$ (7). Moreover, widely-used biomarkers, such as TEX_{86} and $U^{k'}_{37}$, are uniquely based on empirical correlations to temperature, and the mechanism (s) driving these correlations is

(are) not well known. In contrast, the relationship of Δ_{47} with temperature is well understood and grounded in thermodynamics. Since most of the temperature reconstructions from the Miocene are based on $U_{37}^{k'}$ (4), new records based on Δ_{47} thermometry during this time allow us to improve the reliability of absolute temperature estimates. Recent improvements in the precision, methods, calibrations, and sample size requirements of Δ_{47} thermometry have made it useful for paleoceanographic applications (e.g. refs. (7, 8)).

Despite being geographically widespread since the Mesozoic and ensuring a euphotic ocean signal due to their reliance on light, the application of Δ_{47} to calcite produced by coccolithophores has received attention by the community only recently (9–14). Two studies on cultured coccolithophores, showed that despite the large vital effects in $\delta^{18}O$ and $\delta^{13}C$, the relationship between coccolith Δ_{47} and temperature appears to be consistent across different species (10, 14). Altogether, available data suggests that the application of Δ_{47} to coccolith samples of mixed species is a reliable indicator of coccolithophores' calcification temperature, which in well-mixed waters, like at high latitudes, likely reflect integrated mixed-layer temperatures during the production season (13).

Here we applied for the first time Δ_{47} thermometry to exceptionally pure (>90%) downcore coccolith calcite from ODP Site 982 in the North Atlantic (Fig. 1) over the past 16 million years (My), including the Mid and Late Miocene. To further evaluate proxy fidelity, we determined Δ_{47} temperatures of a monospecific *Coccolithus pelagicus* sediment trap in the nearby Iceland Sea for which remote sensed temperatures are well-constrained. We additionally estimated sea surface temperatures (SSTs) by applying widely-used calibrations (15–17) to $U_{37}^{k'}$ indexes measured on the same downcore ODP Site 982 samples, as a comparison to our coccolith Δ_{47} calcification temperature record. Although alkenones and coccoliths are both produced by coccolithophores, we find significant differences in absolute temperatures amongst these proxies throughout the analyzed time interval. This study presents North Atlantic coccolith Δ_{47} temperature reconstructions that for the first time fit with Miocene modeling studies showing a modest, rather than an extreme high latitude warmth, and highlights the importance of continuous re-evaluation of our understanding of both new and well-established proxies.

Results and Discussion

Coccolith clumped isotope temperatures

The Δ_{47} temperature of the monospecific *C. pelagicus* sediment trap in the Iceland Sea (7.41 ± 4.4 °C; 95% confidence interval, CI; Fig. 2a) closely agrees with the AVHRR satellite-derived production temperatures of 6.74 °C (18). This further supports the applicability of coccolith Δ_{47} as a reliable proxy of calcification temperatures. Our North Atlantic downcore Δ_{47} temperatures are from 91-98% pure and well preserved coccolith separations (2-10 µm; Fig. 3), and show Mid-Miocene peak temperatures of 18.3 ± 5.0 °C and a gradual cooling of 9.0 °C throughout the studied period (Fig. 2a). Absolute Δ_{47} temperatures are similar between the pure coccolith (2-10 µm) and the <11 µm size fractions. This implies that at this site and since the Mid-Miocene, neither foraminifera fragments (10-11 µm; SI Appendix Fig. S1) nor potentially diagenetically-formed small unidentifiable carbonate <2 µm in size significantly affected the calculated temperatures.

Coccolith Δ_{47} suggest a 10°C colder North Atlantic compared to $U^{k'}_{37}$

Negligible cold bias in the coccolith Δ_{47} record

Several lines of evidence suggest that the Δ_{47} temperatures reflect the primary calcification temperature of coccoliths with negligible influence from variable vital effects or diagenetic overprinting. The samples of the fraction 2-10 µm not only consist of unprecedented highly pure (91-98%) coccoliths, but are also dominated (78-93%) by the same *Reticulofenestra* taxa that produce alkenones (SI Appendix Fig. S2). Given the dominance of these species, we expect that any cold bias in coccolith Δ_{47} temperatures due to assemblage variability remained well-below analytical detection. Despite the consistency in coccolith Δ_{47} temperature dependence across species (10, 14), and the so far proven reliability of Δ_{47} calcification temperatures from mixed species (13), lateral advection of other coccoliths typical of more subpolar areas, like *C. pelagicus,* could introduce a cold bias. We evaluated this potential cold bias in Δ_{47} temperatures from the sample with the highest contribution of this species (10.6%) at ~14 Ma and show that

158 this contamination would lead to a temperature underestimation of less than ~1 °C (SI Appendix
159 Note S1).
160 A cold temperature bias could in principle be introduced by the presence of diagenetic calcite
161 formed at the seafloor. However, our data and analyses suggest small contributions of
162 authigenic carbonate in our coccoliths (SI Appendix Note S2). Using estimates of the maximum
163 amount of authigenic calcite in our samples (2.8-8.1 %, SI Appendix Table S1, Fig. S3 and S4),
164 the Δ_{47} diagenesis model of Stolper et al. (19) predicts cold biases of <2 °C (SI Appendix Fig.
165 S5), which we consider the uppermost limit on the potential influence of diagenesis on Δ_{47}
166 temperatures. Moreover, the model indicates that post-burial diagenesis would lead to larger
167 offsets compared to the alkenone data in older samples, as these samples would undergo more
168 extensive diagenetic alteration (SI Appendix Fig. S5). However, this pattern is not reflected in
169 our data, where Δ_{47} offsets relative to alkenone temperatures are consistent throughout the
170 record. A negligible cold bias from authigenic carbonate in our record is further supported by the
171 Sr/Ca values of our pure coccolith fractions (SI Appendix Table S2), which are in the range of
172 those typical of cultured coccoliths, sediment traps and sediment cores (20), and are 100 fold
173 higher than those expected from abiogenic calcite (21). Scanning Electron Microscopy (SEM)
174 show evidence of some dissolution in all samples. To date, there is no evidence that partial
175 dissolution bias Δ_{47} of coccoliths. Although further research might be needed to confirm this
176 general conclusion, coccoliths are single, chemically homogeneous crystals (22), generated
177 within one hour (23), and are protected by polysaccharides (24, 25). This makes it unlikely that
178 partial removal of calcite from etching in coccoliths would cause significant alteration of their Δ_{47}
179 values.
180 Δ_{47} calcification temperatures over the last 16 My are on average ~9 °C colder than those
181 derived from $U^{k'}_{37}$ from the same samples (Fig. 2a, b). The above discussion of potential cold
182 bias sources in our coccolith Δ_{47} calcification record shows that, if present, they could only
183 explain a small part of this ~9 °C difference (smaller than current Δ_{47} analytical errors). We
184 propose, in agreement with the coccolith core top Δ_{47} study of Mejia et al. (13), that such
185 differences can be at least in part explained by the calibration approaches applied to these
186 proxies.

Could alkenone records overestimate North Atlantic temperatures?

If alkenones were produced under the same conditions (i.e. season, depth, light, nutrients, growth phase) during which coccolithophores calcify, we would expect similar absolute temperature estimates from both proxies. However, despite sharing similar trends and being correlated (Fig. 2, SI Appendix Fig. S6), coccolith Δ_{47} calcification temperatures are significantly colder than alkenone temperatures estimated using calibrations based on regressions of $U^{k'}_{37}$ against SSTs (15, 16) (Fig. 2a, b). Widely-used alkenone calibrations used for temperature reconstructions in the North Atlantic are based on annual (core top (15)) and warm season (August-October; Bayspline (16)) temperatures at 0 m. In contrast, Δ_{47} calibrations are based on actual or inferred temperatures during carbonate formation. Consequently, in places or time intervals in which coccolith biomineralization (and alkenone formation) occurs at depth and/or during cooler seasons, the application of such calibrations to $U^{k'}_{37}$ records is expected to overestimate SSTs, and produce warmer estimates than actual calcification temperatures derived from Δ_{47}. We suggest that since the Mid-Miocene, absolute calcification temperatures at ODP Site 982 are better represented by coccolith Δ_{47}, and that the application of the widely-used calibrations based on regressions of mean annual or warm season SSTs to alkenones (15, 16) likely lead to overestimated temperatures for the season and depth of production.

Coccolithophore production in the modern North Atlantic is the highest between the colder winter and spring seasons (26), and there is no evidence for peak production during the warmer August-October period (26–31). Moreover, coccolith Δ_{47} was suggested to represent mixed layer, rather than surficial temperatures for the same site (13). While the maximum temperature effect of production deeper than the sea surface is relatively small for this location, due to its weak thermocline (maximum of ~1.6 °C, assuming deepest production at 100 m; SI Appendix Note S3, Table S3), the maximum temperature effect of applying alkenone calibrations based on SSTs outside the actual season of production is larger (up to 3 °C; SI Appendix Note S4, Table S4). For the Mid-Holocene ODP Site 982, published alkenone-derived temperatures using the core-top (15) and Bayspline (16) calibrations were up to 5.9 °C warmer than both SSTs during the season of production and coccolith Δ_{47} calcification temperatures (13). Together, for the modern North Atlantic, the maximum effects of applying alkenone calibrations based on 1) SSTs rather than on temperatures at depth of production and 2) SSTs during a warmer season

than that of production, can explain up to 78% of the difference in published Mid-Holocene absolute temperature estimates between coccolith Δ_{47} and alkenones (13). An increasingly stratified North Atlantic during warmer past intervals, or a larger difference of temperatures between seasons, could exacerbate the depth and the season of production effects, therefore increasing differences of estimated temperatures between proxies.

An analog approach to Δ_{47} calibrations is that of alkenone calibrations based on culture temperatures, and we would therefore expect estimated absolute values to be similar. When applying culture calibrations, the *Emiliania huxleyi* (strain 55a) batch culture calibration (17) is the most widely applied, and it generally agrees with calibrations based on SSTs (15, 16). Yet, several other culture studies on different strains of *E. huxleyi* and *Gephyrocapsa oceanica* show different alkenone unsaturation calibrations to growth temperatures (32). When applied to our $U_{37}^{k'}$ dataset, there are up to 8.0 °C differences among these culture experiments and surprisingly, all yield even warmer temperatures than the modern SST and the published coccolith Δ_{47} core top temperature (13) (Fig. 2a, SI Appendix Table S5). These large differences in the sensitivity of $U_{37}^{k'}$ to cultured temperature highlight the need to improve our knowledge on aspects like the utility of synthesizing alkenones, cellular production pathways, and all possible non-thermal mechanisms that may, together with temperature, also influence this proxy. This would help clarifying the absolute temperature estimates and which calibrations are most appropriate for a given oceanographic setting.

An alternative empirical alkenone calibration based on season of production temperatures at depth, rather than on annual or August-October SSTs, was recently proposed (13). This calibration employs a subset of sites from the broader global alkenone calibration set (16), for which the season and depth of production can be inferred to be similar to those at geographically proximal core top sites for which coccolith Δ_{47} were determined (13). This empirical calibration regresses these $U_{37}^{k'}$ values to the temperatures at the depth and season of production inferred from the core top coccolith Δ_{47} dataset (13). Applying this calibration to our ODP 982 $U_{37}^{k'}$ values, we obtain absolute alkenone-derived growth temperatures that agree much better with the absolute values of our coccolith Δ_{47} record (Fig. 4). The same is valid when this calibration is applied to the higher resolution ODP Site 982 $U_{37}^{k'}$ Miocene values of the study of Super et al. (33), which decreases average alkenone temperatures by ~6.6 °C (Fig. 4).

Although we recognize that a much larger dataset would be required to make such a calibration more robust and widely applicable for reconstructions, these results suggests that when depth and season of production of coccolithophorids are considered in the calibrations, a large part of the observed discrepancies in absolute values between coccolith Δ_{47} and alkenone proxies are resolved. This adds confidence to our conclusion from coccolith Δ_{47} that the euphotic North Atlantic was likely ~9 °C colder than what alkenone temperatures from conventional calibrations (15, 16) suggest. The coccolith Δ_{47} temperatures and recalibrated alkenone temperatures are also more compatible with the deep-sea benthic foraminifera Δ_{47} temperature reconstructions of (8) for ODP 982, a location proximal to sites of deep-water formation. For the Miocene, most available temperature records are alkenone-based (4). If similar findings of cooler production temperatures were reproduced at other high latitude sites, they would have important implications in our understanding of future high latitude amplification.

Alkenone and coccolith Δ_{47} temperatures can be readily compared because they derive from the same organism. Detailed comparison of absolute coccolith Δ_{47} temperatures with other records from proxies based on other organisms, like $TEX_{86,}$ would require a thorough analysis not only of calibrations but also poorly constrained differences in the ecology of the biomarker producers which is beyond the scope of this paper. Miocene absolute TEX_{86} temperatures at our site were found to be generally similar (or even slightly colder) to those at a location 14.7° further south in the subtropical gyre (33), and more consistent with the coldest endmembers of our alkenone estimates (SI Appendix Fig. S7). Similar temperatures at ODP Site 982 and at the subtropical gyre would be possible under extreme high latitude amplification. Alternatively, it is also possible that there was still a latitudinal thermal gradient between these sites that cannot be discerned by TEX_{86} at these locations or time intervals, potentially due to similar challenges in the attribution of the production depth and season.

Modest, not extreme northern high latitude amplification over the Mid-Late Miocene: perspectives for model-coccolith Δ_{47} data comparisons

Our coccolith Δ_{47} record provides new estimates of North Atlantic absolute temperatures from the mixed layer winter-spring season since the Mid-Miocene, and represents a new target for paleoclimate model-data comparisons. For locations with a strong seasonal temperature

278 cycle, robust model-data comparisons require a clear attribution of season, but also of depth of
279 the signal. Our analysis suggests these criteria are well met for coccolith Δ_{47} calcification
280 temperatures in the North Atlantic, because they are coherent with the known production
281 regime. This Δ_{47} temperature record is the first to agree (for Late Miocene), and the closest to
282 match (for Middle Miocene) modeling studies (Fig. 5), including that of the first attempt of a
283 Miocene multi-model comparison (4).
284 The flattening of the Miocene latitudinal thermal gradient and extreme high latitude
285 amplification (1), especially for the warmest Mid-Miocene, has been a major paleoclimate
286 conundrum because climate models struggle to achieve such warm high latitude temperatures
287 (e.g. ref. (4, 34, 35))), suggesting complications with proxy interprations or missing physics in
288 climate models. The recent study that concluded a persistent high latitude amplification in the
289 Pacific since the Late Miocene based their calculations in comparisons of their multiproxy
290 Western Pacific Warm Pool stack with North Pacific alkenone-derived SSTs (36). The latter
291 absolute values have only been sucessfully simulated by one model (COSMOS) that also
292 significantly overestimates tropical temperatures (4). Therefore, it is possible that these
293 alkenone-based high latitude reconstructions are also warm-biased and therefore not approriate
294 to calculate amplification. Our comparatively smaller coccolith Δ_{47} dataset hampers the
295 calculation of reliable high latitude amplification from similar comparisons to tropical
296 temperatures as conducted by Liu et al. (36). However, increasing the resolution of coccolith Δ_{47}
297 in high latitudes would allow them in the future.
298 Miocene extreme polar amplification has been best simulated using CO_2 concentrations
299 around the maximum values (or higher) than those suggested by proxies (4, 35), but high
300 latitude warmth in places like the North Atlantic (and the high latitude southern hemisphere)
301 continues to fall short in model simulations, while tropical temperatures tend to be
302 overestimated. The best fit with current proxy data for the Late Miocene was achieved with the
303 NorESM-L model set at 560 ppm of CO_2 (higher than proxy estimates), which includes an
304 improved representation of cloud microphysics and led to the best capture of polar amplification
305 during the Eocene (37). Simulations from this model show latitudinal temperature gradients
306 between ODP Site 982 and the Eastern Equatorial Pacific (EEP) of ~14.6 °C. Assuming that
307 alkenones represent well temperatures of the EEP (38), latitude temperature gradients for the

Late Miocene calculated using our North Atlantic coccolith Δ_{47} (~13.5 °C) are much more consistent with climate models than those derived from the average of all other proxies available for our location (~4.7 °C including our alkenone record) (Fig. 5). For the Mid-Miocene, even CO_2 concentrations of 850 ppm were not able to reproduce the even flatter temperature gradient shown by proxy data (best fitting model: HadCM3L; (4)), and EEP temperatures were overestimated by almost 5 °C. Lower CO_2 concentrations improve tropical temperature simulations, but in these simulations the North Atlantic is even colder than the modern ocean. The multiple optimization Earth System model of Mid-Miocene based on cGENIE required CO_2 concentrations as high as1120 ppm to achieve the highest North Atlantic temperatures without overestimating tropical temperatures, simulating a latitudinal thermal gradient of 15.8 °C. While the gradient between EEP alkenone-derived temperatures and our North Atlantic coccolith Δ_{47} record is more similar to this model (11.2 °C), that suggested by other published proxies is negligible (2.7 °C) (Fig. 5). This analysis shows that coccolith Δ_{47} calcification temperatures are more consistent with modeled Late and Mid Miocene latitude thermal gradients and suggest a lower degree of high latitude amplification than that inferred from other proxy data.

The debate over high latitude amplification exists for other time intervals like the Eocene, although new modelling attemps have been able to better reproduce high latitude warmth (37, 39). During the Eocene, however, it was paleocenographic forcing, rather than CO_2, that may have contributed more to high latitude warmth compared to the Miocene (4). We suggest that it is worth exploring coccolith Δ_{47} as a proxy to test high latitude amplification in other regions and also further back in time. If the more modest Mid and Late Miocene high latitude warmth shown by our coccolith Δ_{47} is reproduced in other high latitudes, the conclusion of modest, not extreme amplification, would provide a more optimistic perspective of high latitude climate response to anthropogeic CO_2 emissions in the future than implied by proxy data in the past, while underscoring the necessity to better understand the mechanisms affecting all existing temperature proxies at different locations and times.

Conclusions

Simulating the extreme high latitude warmth suggested by widely-used temperature proxies during past warm intervals, especially during the Miocene, has proven to be very

challenging for the climate modeling community. This first downcore record of pure coccolith Δ_{47} calcification temperatures in the North Atlantic over the Mid to Late Miocene, show absolute values that agree much better with model simulations, suggesting that the North Atlantic was ~9° C colder than what other proxies showed in the past. The careful evaluation of potential cold biases of this record shows that these likely remained below analytical uncertainties, and suggests that for this location and time coccolith Δ_{47} may be more reliable that other proxies calibrated to SST during warmer than actual production seasons. Colder Northern high latitudes that better agree with Miocene climate models also highlight the need for a continuous reexamination of our interpretation of both new and more established proxies, so as to achieve not only reliable temperature trends, but also accurate absolute values. If this less extreme high latitude warmth is reproduced in other high latitudes or other warm intervals, the currently accepted paradigm of extreme flattening of the temperature gradient would likely require reevaluation, and would offer a less catastrophic perspective of climate response to increasingly anthropogenic CO_2.

Methods

Oceanographic setting in the North Atlantic

ODP Site 982 is located in the North Atlantic (Rockall Plateau, 57° 31.002' N and 15° 51.993' W; water depth 1134 m; Fig. 1). Its paleo-geographical location has not changed significantly in the last 15 My (1) and sediment is carbonate rich (86%), making it ideal for achieving coccolith pure samples. We used nine samples with depths ranging between 43.99 and 524.55 m (mcd), corresponding to ages between 1.99 and 16 Ma. The age model until 5 Ma was based on the correlation of benthic foraminiferal $\delta^{18}O$ from ODP Site 982 and those of the LR04 stack, while after 8 Ma, it was based in biostratigraphy (1). Between 5 and 8 Ma, we used the latest age model derived from high resolution XRF core scanning data and benthic foraminifera $\delta^{18}O$ and $\delta^{13}C$ astrochronology (40). We also used a sediment trap sample from the Iceland Sea (70.23° N; 9.75° W; 1884 m) (18), which in July 1999 registered the largest surface bloom ever recorded in this area, containing 99% of the subpolar north Atlantic *C. pelagicus*.

Alkenone thermometry

Bulk sediments were freeze-dried and the total lipid extract (TLE) was obtained via Accelerated Solvent Extraction (ASE) following methods detailed in Mejia et al. (13) After saponification using a 0.5 M solution of KOH in MeOH:H_2O (95:5), the neutral alkenone-containing fraction was extracted with toluene, and further purified via silica gel column chromatography. The ketone fraction containing alkenones was measured at ETH Zürich using a Thermo Scientific Trace 1310 Gas Chromatograph (GC) coupled to a flame ionization detector, as shown in Guitián et al. (41) The $U_{37}^{k'}$ ratio was calculated from the abundance of $C_{37:2}$ and $C_{37:3}$, from which SSTs were derived using the core top (15), the 55a *Emiliania huxleyi* batch culture (17) and the Bayspline (16) calibrations. In-house alkenone standard repeated measurements yielded a precision of 0.012 $U_{37}^{k'}$ units (0.36°C calculated with the core top (15) calibration).

Coccolith clumped isotope thermometry

Sample processing

After lipid extraction for alkenone analyses, samples were microfiltered in ammonia solution (0.5%) at 11 µm to obtain a coccolith-enriched fraction. To avoid potential interference from organics during Δ_{47} analyses, we eliminated the remaining organic matter using buffered 10% H_2O_2, as described in Mejia et al. (13). No effects in coccolith stable or clumped isotopes were reported using this method (13). Since diagenetic processes are more prone to happen in the smallest fragments, whose source is also impossible to identify, we used centrifugation techniques (seven repetitions at 2300-2800 RPM for 2 minutes) to remove the < 2 µm size fraction (42). We then produced a pure coccolith fraction (2-10 µm) by extensive microfiltration at 2 at 10 µm. The remaining 10-11 µm size fraction showed enrichment in fragments of foraminifera (SI appendix Fig. S1). Coccolith purity of the 2-10 µm fractions and species' assemblages were determined using light microscopy. To test whether small calcite of unidentifiable origin (<2 µm) and large calcite (10-11 µm) have a significant effect in coccolith Δ_{47} temperatures, a small aliquot from the extracted bulk sediment was sieved at 11 µm using

ethanol, and then oxidized with H_2O_2 as described above. Before Δ_{47} analysis, all samples were rinsed with Mili-Q, dried at 50°C and homogenized.

Evaluation of diagenetically-sourced cold bias

The presence of abiogenic calcite produced at depth and at colder temperatures compared to the original coccolith signal can introduce a cold bias in Δ_{47} temperatures. The degree of secondary overgrowth on coccoliths was evaluated both by trace element analyses and by scanning electron microscopy (SEM). We used weak acetic acid (0.4 M) to dissolve 50-100 µg of the pure coccolith (2-10 µm) and the <2 µm size fractions. Sr, Mg and Al/Ca ratios were determined using an Agilent 8800 Triple Quadrupole ICP-MS at ETH Zürich, following the intensity ratio calibration described in (20).

To date, there are no techniques able to quantify authigenic calcite in coccoliths. Most studies provide only qualitative descriptions of calcite preservation. Instead, here we produced a very conservative estimate of the maximum diagenesis effect, by applying the geometrically-calculated coccolith volume plots of Young and Ziveri (43) to calculate the % volume affected from the % of authigenic overgrown area obtained by SEM. Then, this was extrapolated from the center to the edge of the coccolith observed in cross-section, assuming a maximum of half of the calcite was affected by diagenesis (SI appendix Table S1). We applied this method to 13-26 single coccoliths for each sample (average of 18 coccoliths per sample). We also determined the maximum potential effect of the degree of diagenesis on our Δ_{47} temperature estimates, by implementing the Δ_{47} diagenesis model of Stolper et al. (19) (SI appendix Fig. S5), which uses the same model construction as the diagenesis models of refs. (44, 45) (details in SI appendix Note S2), and applied it to our ODP Site 982 coccoliths.

Clumped isotope measurements and temperature estimates

Measurements were conducted using a Kiel IV-Thermo Scientific MAT 253 at ETH Zürich, following the LIDI protocol (46), and the procedures described in Mejia et al. (13), including a PoraPakQ trap (–40 °C) to eliminate residual halo/hydrocarbon and reduced sulfur compounds. Nine to 21 replicates of ~110 µg carbonate were measured depending on sample availability. Measurements were conducted over a period of 18 months, using the carbonate standardization scheme based on ETH-1 (Δ_{47}=0.2052‰), ETH-2 (Δ_{47}= 0.2085‰), and ETH-3 (Δ_{47}=0.6132‰) standards (47). Long term external reproducibility was monitored using the

standard IAEA C2 (standard deviation: $\delta^{13}C$ = 0.02‰, $\delta^{18}O$ = 0.03‰; Δ_{47}=0.03‰). Data processing was carried out with the software Easotope (48). Measurements with Δ_{48} offset > 2 and 49 parameter values > 2 ‰ were eliminated as considered affected by contamination (48).

As demonstrated by the core top coccolith Δ_{47} study (13), the application of abiogenic Δ_{47} calibrations to coccolith samples should be avoided, as they derive too cold temperatures that are found at water depths at which coccolithophores would not be able to photosynthesize. Similarly, the recent coccolith culture Δ_{47} study of (14) suggests that coccoliths have a systematic offset from the generalized calibration that includes abiogenic samples (49), and that there is a consistent relationship between growth temperature and Δ_{47} across different species (10, 14). Here we use this culture coccolith Δ_{47} calibration (14) to calculate calcification temperatures from Δ_{47} of ODP Site 982 coccoliths. The application of this coccolith calibration leads to absolute temperature values and trends that are remarkably similar to those obtained using the foraminifera calibration of (7) (SI Appendix Fig. S8). Further data on both cultured coccoliths and foraminifera would clarify if the magnitude of the offset to abiogenic carbonates may be shared by these biogenic carbonates extremely important for paleoceanography.

Acknowledgements

This project has received funding from the European Union's Horizon 2020 research and innovation programme under the Marie Sklodowska-Curie gran agreement 795053, from ETH Zurich Core funding, and from MARUM through DFG Germany's Excellence Strategy, Cluster of Excellence "The Ocean Floor - Earth's Uncharted Interface' (EXC-2077, Project 390741603). We thank laboratory technician Stewart Bishop, laboratory assistants Manuel Walde and Sarah Rowan, Steve Maganini, Dorinda Ostermann and Susumu Honjo for providing the sediment trap sample, and Iván Hernández-Almeida for assistance in depth-integrated variable calculations.

Supporting information

Supporting information is available in the online version of the paper. Correspondence and requests should be addressed to L.M.M

References

1. T. D. Herbert, *et al.*, Late Miocene global cooling and the rise of modern ecosystems. *Nat Geosci* **9**, 843–847 (2016).

2. Z. Liu, *et al.*, Global cooling during the eocene-oligocene climate transition. *Science (1979)* **323**, 1187–1190 (2009).

3. T. Westerhold, *et al.*, An astronomically dated record of Earth's climate and its predictability over the last 66 million years. *Science (1979)* **369**, 1383–1388 (2020).

4. N. J. Burls, *et al.*, Simulating Miocene Warmth: Insights From an Opportunistic Multi-Model Ensemble (MioMIP1). *Paleoceanogr Paleoclimatol* **36**, e2020PA004054 (2021).

5. M. Steinthorsdottir, *et al.*, The Miocene: The Future of the Past. *Paleoceanogr Paleoclimatol* **36**, e2020PA004037 (2021).

6. E. A. Schauble, P. Ghosh, J. M. Eiler, Preferential formation of 13C-18O bonds in carbonate minerals, estimated using first-principles lattice dynamics. *Geochim Cosmochim Acta* **70**, 2510–2529 (2006).

7. N. Meinicke, M. A. Reimi, A. C. Ravelo, A. N. Meckler, Coupled Mg/Ca and Clumped Isotope Measurements Indicate Lack of Substantial Mixed Layer Cooling in the Western Pacific Warm Pool During the Last ~5 Million Years. *Paleoceanogr Paleoclimatol* **36**, e2020PA004115 (2021).

8. A. N. Meckler, *et al.*, Cenozoic evolution of deep ocean temperature from clumped isotope thermometry. *Science (1979)* **377**, 86–90 (2022).

9. A. J. Drury, C. M. John, Exploring the potential of clumped isotope thermometry on coccolith-rich sediments as a sea surface temperature proxy. *Geochemistry, Geophysics, Geosystems* **17**, 4092–4104 (2016).

10. A. Katz, M. Bonifacie, M. Hermoso, P. Cartigny, D. Calmels, Laboratory-grown coccoliths exhibit no vital effect in clumped isotope (Δ47) composition on a range of geologically relevant temperatures. *Geochim Cosmochim Acta* **208**, 335–353 (2017).

11. A. K. Tripati, *et al.*, 13C-18O isotope signatures and "clumped isotope" thermometry in foraminifera and coccoliths. *Geochim Cosmochim Acta* **74**, 5697–5717 (2010).

12. M. Tagliavento, C. M. John, L. Stemmerik, Tropical temperature in the Maastrichtian Danish Basin: Data from coccolith Δ47 and δ18O. *Geology* **47**, 1074–1078 (2019).

13. L. M. Mejía, *et al.*, Clumped isotopes in globally distributed Holocene coccoliths reveal their habitat depth. *Earth Planet Sci Lett* **619**, 118313 (2023).

14. A. J. Clark, I. Torres-Romero, M. Jaggi, S. M. Bernasconi, H. M. Stoll, Coccolithophorids precipitate carbonate in clumped isotope equilibrium with seawater. *Preprint egusphere 2023-2581* (2023). https://doi.org/10.5194/egusphere-2023-2581.

15. P. J. Müller, G. Kirst, G. Ruhland, I. Von Storch, A. Rosell-Melé, Calibration of the alkenone paleotemperature index UK'37 based on core-tops from the eastern South Atlantic and the global ocean (60°N-60°S). *Geochim Cosmochim Acta* **62**, 1757–1772 (1998).

16. J. E. Tierney, M. P. Tingley, BAYSPLINE: A New Calibration for the Alkenone Paleothermometer. *Paleoceanogr Paleoclimatol* **33**, 281–301 (2018).

17. F. G. Prahl, L. A. Muehlhausen, D. L. Zahnle, Further evaluation of long-chain alkenones as indicators of paleoceanographic conditions. *Geochim Cosmochim Acta* **52**, 2303–2310 (1988).

18. V. Cullen, Ed., Woods Hole Oceanographic Institution. Iceland Sea carbonate flux increases dramatically. *In 2001 Annual Report. (V. Cullen, 2001)* [Preprint].

19. D. A. Stolper, J. M. Eiler, J. A. Higgins, Modeling the effects of diagenesis on carbonate clumped-isotope values in deep- and shallow-water settings. *Geochim Cosmochim Acta* **227**, 264–291 (2018).

20. L. M. Mejía, *et al.*, Effects of midlatitude westerlies on the paleoproductivity at the Agulhas Bank slope during the penultimate glacial cycle: Evidence from coccolith Sr/Ca ratios. *Paleoceanography* **29** (2014).

21. F. M. Richter, Y. Liang, The rate and consequences of Sr diagenesis in deep-sea carbonates. *Earth Planet Sci Lett* **117**, 553–565 (1993).

22. H. Stoll, *et al.*, Insights on coccolith chemistry from a new ion probe method for analysis of individually picked coccoliths. *Geochemistry, Geophysics, Geosystems* **8**, Q06020 (2007).

23. L. M. Mejía, *et al.*, Controls over $\delta^{44/40}$Ca and Sr/Ca variations in coccoliths: New perspectives from laboratory cultures and cellular models. *Earth Planet Sci Lett* **481** (2018).

24. T. Hassenkam, A. Johnsson, K. Bechgaard, S. L. S. Stipp, Tracking single coccolith dissolution with picogram resolution and implications for CO2 sequestration and ocean acidification. *Proc Natl Acad Sci U S A* **108**, 8571–8576 (2011).

25. T.-C. Chiu, W. S. Broecker, Toward better paleocarbonate ion reconstructions: New insights regarding the CaCO3 size index. *Paleoceanography* **23**, PA2216 (2008).

26. M. J. Behrenfeld, S. C. Doney, I. Lima, E. S. Boss, D. A. Siegel, Annual cycles of ecological disturbance and recovery underlying the subarctic Atlantic spring plankton bloom. *Global Biogeochem Cycles* **27**, 526–540 (2013).

27. A. T. C. Broerse, P. Ziveri, J. E. Van Hinte, S. Honjo, Coccolithophore export production, species composition, and coccolith-CaCO3 fluxes in the NE Atlantic (34 °N 21 °W and 48 °N 21 °W). *Deep Sea Res 2 Top Stud Oceanogr* **47**, 1877–1905 (2000).

28. A. Rosell-Melé, F. G. Prahl, Seasonality of UK'37 temperature estimates as inferred from sediment trap data. *Quat Sci Rev* **72**, 128–136 (2013).

29. A. Rosell-Melé, P. Comes, P. J. Müller, P. Ziveri, Alkenone fluxes and anomalous UK'37 values during 1989-1990 in the Northeast Atlantic (48°N 21°W). *Mar Chem* **71**, 251–264 (2000).

30. A. Filippova, M. Kienast, M. Frank, R. R. Schneider, Alkenone paleothermometry in the North Atlantic: A review and synthesis of surface sediment data and calibrations. *Geochemistry, Geophysics, Geosystems* **17**, 1370–1382 (2016).

31. A. Mignot, R. Ferrari, H. Claustre, Floats with bio-optical sensors reveal what processes trigger the North Atlantic bloom. *Nat Commun* **9**, 1–9 (2018).

32. W. J. D'Andrea, S. Theroux, R. S. Bradley, X. Huang, Does phylogeny control U37K-temperature sensitivity Implications for lacustrine alkenone paleothermometry. *Geochim Cosmochim Acta* **175**, 168–180 (2016).

33. J. R. Super, *et al.*, Miocene Evolution of North Atlantic Sea Surface Temperature. *Paleoceanogr Paleoclimatol* **35**, e2019PA003748 (2020).

34. A. Goldner, N. Herold, M. Huber, The challenge of simulating the warmth of the mid-Miocene climatic optimum in CESM1. *Climate of the Past* **10**, 523–536 (2014).

35. K. A. Crichton, A. Ridgwell, D. J. Lunt, A. Farnsworth, P. N. Pearson, Data-constrained assessment of ocean circulation changes since the middle Miocene in an Earth system model. *Climate of the Past* **17**, 2223–2254 (2021).

36. X. Liu, M. Huber, G. L. Foster, A. Dessler, Y. G. Zhang, Persistent high latitude amplification of the Pacific Ocean over the past 10 million years. *Nature Communications 2022 13:1* **13**, 1–14 (2022).

37. D. J. Lunt, *et al.*, DeepMIP: Model intercomparison of early Eocene climatic optimum (EECO) large-scale climate features and comparison with proxy data. *Climate of the Past* **17**, 203–227 (2021).

38. G. Rousselle, C. Beltran, M. A. Sicre, I. Raffi, M. De Rafélis, Changes in sea-surface conditions in the Equatorial Pacific during the middle Miocene–Pliocene as inferred from coccolith geochemistry. *Earth Planet Sci Lett* **361**, 412–421 (2013).

39. J. Zhu, C. J. Poulsen, J. E. Tierney, Simulation of Eocene extreme warmth and high climate sensitivity through cloud feedbacks. *Sci Adv* **5** (2019).

40. A. J. Drury, T. Westerhold, D. Hodell, U. Röhl, Reinforcing the North Atlantic backbone: revision and extension of the composite splice at ODP Site 982. *Climate of the Past* **14**, 321–338 (2018).

41. J. Guitián, *et al.*, Midlatitude Temperature Variations in the Oligocene to Early Miocene. *Paleoceanogr Paleoclimatol* **34**, 1328–1343 (2019).

42. H. Zhang, C. Liu, L. M. Mejía, H. Stoll, Technical note: Accelerate coccolith size separation via repeated centrifugation. *Biogeosciences* **18**, 1909–1916 (2021).

43. J. R. Young, P. Ziveri, Calculation of coccolith volume and its use in calibration of carbonate flux estimates. *Deep Sea Res 2 Top Stud Oceanogr* **47**, 1679–1700 (2000).

44. F. M. Richter, D. J. DePaolo, Numerical models for diagenesis and the Neogene Sr isotopic evolution of seawater from DSDP Site 590B. *Earth Planet Sci Lett* **83**, 27–38 (1987).

45. D. P. Schrag, D. J. DePaolo, F. M. Richter, Oxygen isotope exchange in a two-layer model of oceanic crust. *Earth Planet Sci Lett* **111**, 305–317 (1992).

46. I. A. Müller, *et al.*, Carbonate clumped isotope analyses with the long-integration dual-inlet (LIDI) workflow: scratching at the lower sample weight boundaries. *Rapid Communications in Mass Spectrometry* **31**, 1057–1066 (2017).

47. S. M. Bernasconi, *et al.*, InterCarb: A Community Effort to Improve Interlaboratory Standardization of the Carbonate Clumped Isotope Thermometer Using Carbonate Standards. *Geochemistry, Geophysics, Geosystems* **22**, e2020GC009588 (2021).

48. C. M. John, D. Bowen, Community software for challenging isotope analysis: First applications of 'Easotope' to clumped isotopes. *Rapid Communications in Mass Spectrometry* **30**, 2285–2300 (2016).

49. M. Daëron, P. Vermeesch, Omnivariant Generalized Least Squares regression: Theory, geochronological applications, and making the case for reconciled Δ47 calibrations. *Chem Geol* **647**, 121881 (2024).

Figures

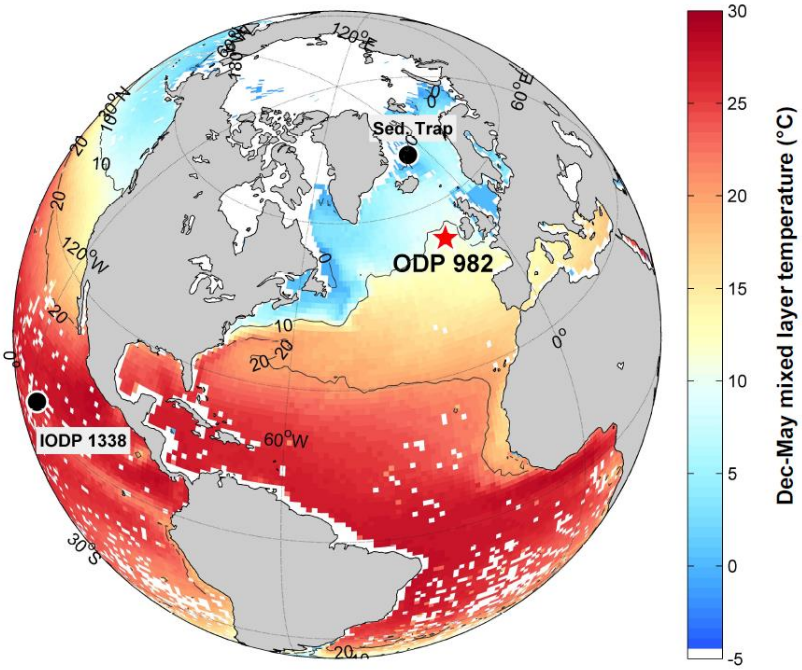

Fig 1. December to May mixed layer depth temperature map with the location of sites discussed in this study. Red star indicates ODP Site 982, from which coccolith clumped isotope and alkenone temperatures were obtained for the last 16 My. Black dots indicate the location of the tropical IODP Site U1338 and the sediment trap in the Iceland sea, the last from which coccolith clumped isotope temperatures were also measured.

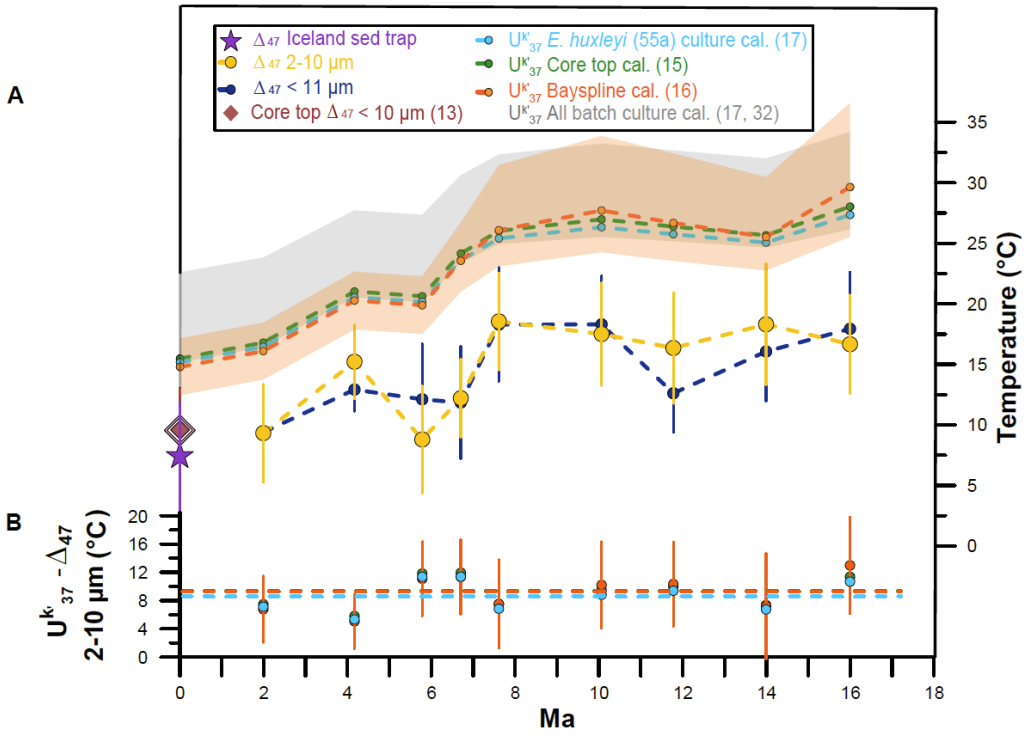

589

590 **Fig 2. Coccolith clumped isotope and alkenone temperature evolution in the North**
591 **Atlantic (ODP Site 982) over the last 16 My. (A)** Δ_{47} calcification temperatures from the pure
592 coccolith 2-10 (yellow) and the < 11 µm (dark blue) size fractions, and alkenone-derived
593 temperatures from the same samples calculated using the core top ((15); green), Bayspline
594 ((16); orange), *E. huxleyi* 55a batch culture ((17); light blue), and ten further culture calibrations
595 (32) (max. and min. values within the gray shaded area). Orange shaded area represents the
596 95% confidence interval (CI) according to the Bayspline calibration. Alkenone temperatures also
597 calculated from the published coretop $U_{37}^{k'}$ value (13) of our same Site. Sediment trap Δ_{47}
598 temperatures from the Iceland Sea *C. pelagicus* sample shown as a purple star. Coccolith Δ_{47}
599 calcification temperatures from a core top (< 10 µm) at our same location ((13): red diamond) fit
600 well modern ocean SSTs (empty pink diamond). Error bars in coccolith Δ_{47} calcification
601 temperatures record denote the 95% CI. **(B)** Average temperature differences between our
602 alkenone-derived records calculated using the core top ((15); green), Bayspline ((16); orange)
603 and *E. huxleyi* 55a batch culture ((17); light blue) calibrations, and the coccolith Δ_{47} record from
604 the pure 2-10 µm size fraction. Horizontal dashed lines denote average temperature differences
605 calculated using results from all samples. Error bars for differences between alkenone
606 Bayspline and coccolith Δ_{47} temperatures are calculated propagating errors from both records.

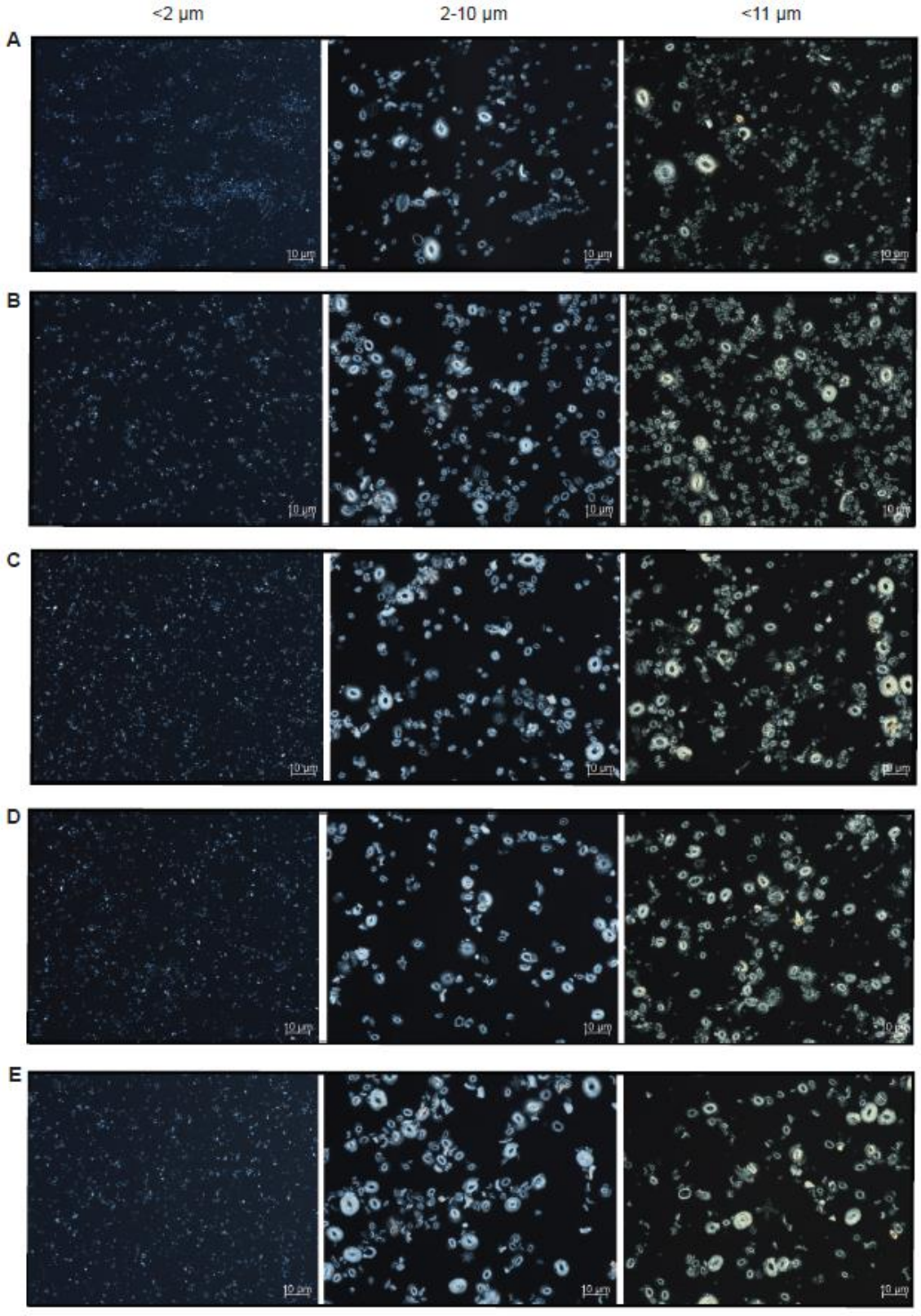

607

608

609

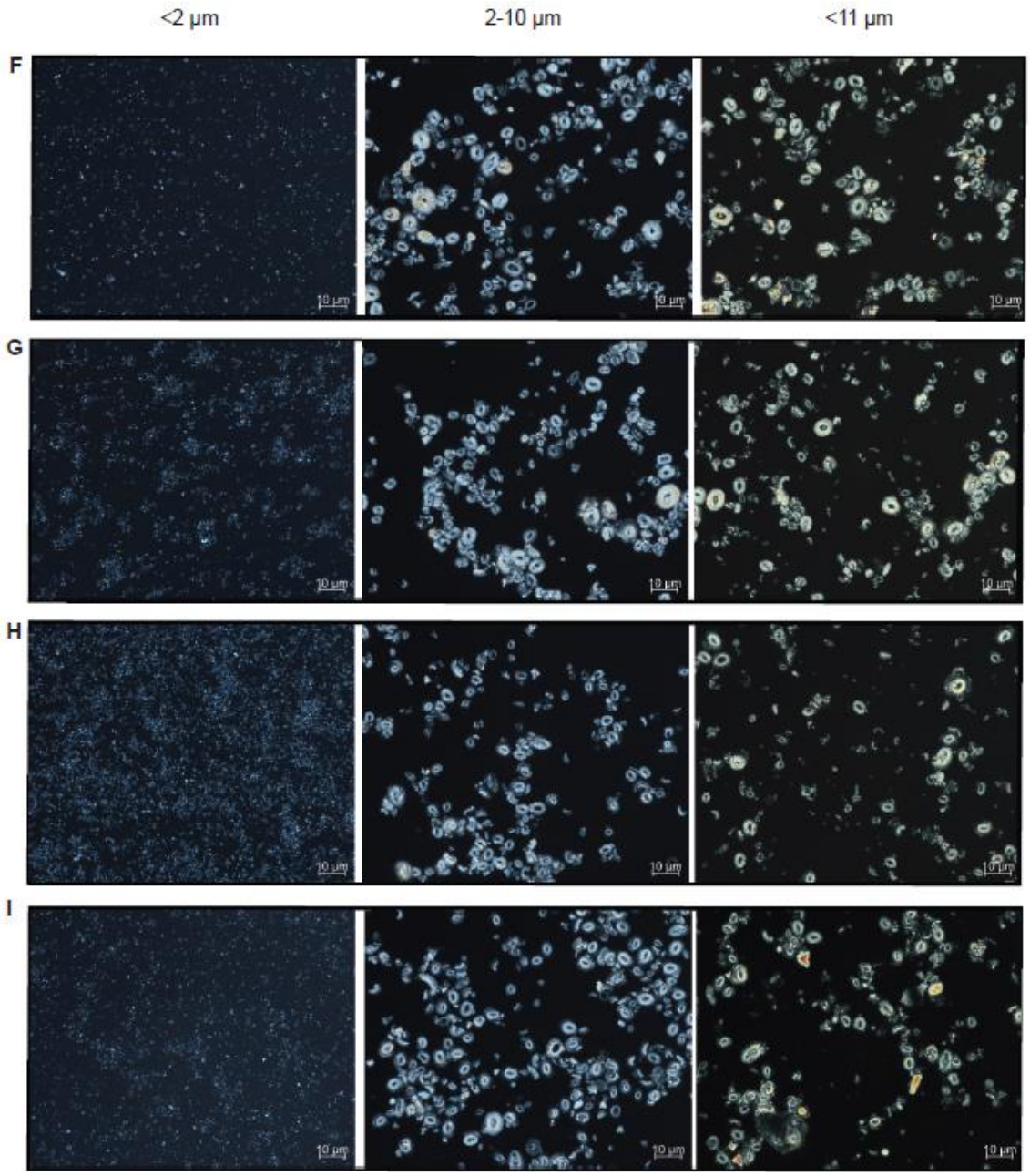

Fig 3. Light microscope images of < 2 µm, pure coccolith (2-10 µm), and <11 µm size fractions of sediment samples from ODP Site 982. (A) 1.99 Ma. **(B)** 4.17 Ma. **(C)** 5.79 Ma. **(D)** 7.61 Ma. **(E)** 6.71 Ma. **(F)** 10.07 Ma. **(G)** 11.78 Ma. **(H)** 13.99 Ma. **(I)** 16 Ma.

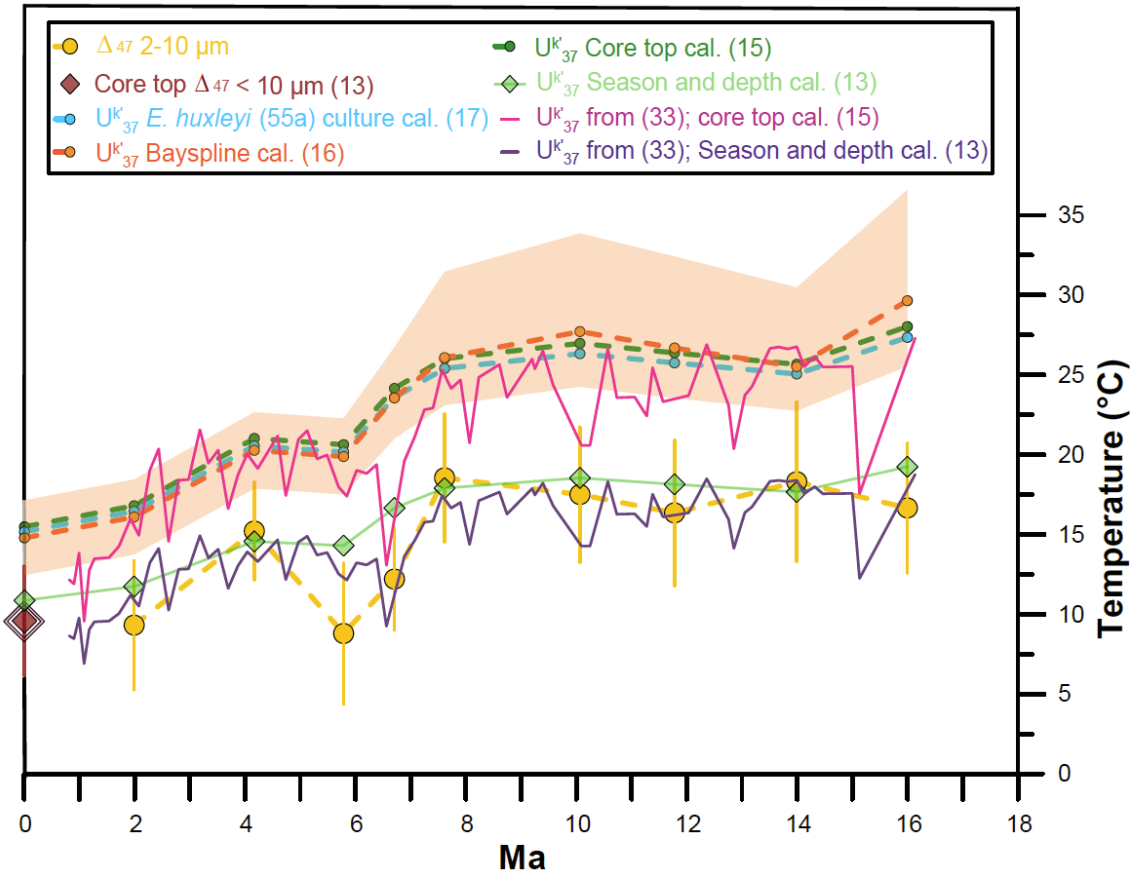

620

621 **Fig 4. ODP Site 982 absolute coccolith clumped isotope calcification temperatures agree**
622 **better with alkenone temperatures calculated using a calibration that considers season**
623 **and depth of production.** Coccolith Δ_{47} calcification temperatures (2-10 µm; yellow), and
624 alkenone-derived temperatures from this study as in Fig. 2, including estimates using the core
625 top ((15); green), Bayspline ((16); orange), *E. huxleyi* 55a batch culture ((17); light blue), and a
626 calibration that considers the season and depth of production ((13); light green diamonds). From
627 the study of Super et al. (33): alkenone temperature record applying the core top ((15); pink line)
628 and a calibration that considers the season and depth of production ((13); purple line). The latter
629 generally agrees with absolute temperatures derived from coccolith Δ_{47} (yellow dots) and those
630 derived from our alkenones calculated using the same season-depth calibration (light green
631 diamonds). Orange shaded area represents the 95% CI according to the Bayspline calibration.
632 Alkenone temperatures also calculated from the published coretop $U_{37}^{k'}$ value (13) of our same
633 site. Coccolith Δ_{47} calcification temperatures from a core top (< 10 µm) at our same location
634 ((13); red diamond) fit well modern ocean SSTs (empty pink diamond). Error bars in coccolith
635 Δ_{47} calcification temperatures record denote the 95% CI.

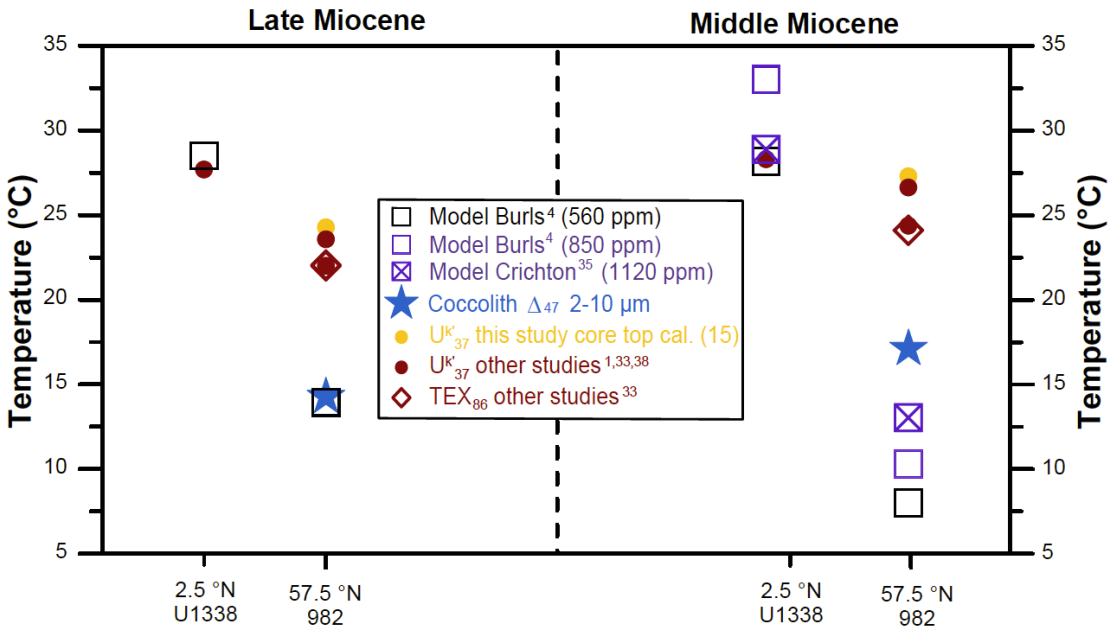

636

637 **Figure. 5. Late and Mid-Miocene latitudinal thermal gradient shown by coccolith clumped**
638 **isotopes, alkenones and model simulations.** While alkenone temperatures calculated using
639 widely-used calibrations suggest a small (Late Miocene) or negligible (Mid-Miocene) latitudinal
640 thermal gradient ((1, 33, 38), and this study), coccolith clumped isotopes and Miocene model
641 simulations (4, 35) suggest a more modest polar amplification and a smaller flattening of the
642 latitudinal thermal gradient.

643

Supporting information for

Modest, not extreme, northern high latitude amplification over the mid to late Miocene shown by coccolith clumped isotopes

Luz María Mejía[a, b*], Stefano M. Bernasconi[a], Alvaro Fernandez[c], Hongrui Zhang[a,d], José Guitián[a,e], Madalina Jaggi[a], Victoria E. Taylor[f], Alberto Perez-Huerta[g], Heather Stoll[a]

[a] Geological Institute, ETH Zürich, Sonneggstrasse 5, ETH, 8092, Zürich, Switzerland
[b] Now at MARUM, University of Bremen, 28359 Bremen, Germany
[c] Instituto Andaluz de Ciencias de la Tierra, Av. de las Palmeras 4, 18100 Armilla, Granada, Spain
[d] Now at Tongji University, Siping Road 1239, Shanghai, China
[e] Now at Centro de Investigación Mariña, Universidade de Vigo, GEOMA, Vigo, 36310, Spain
[f] Department of Earth Science, University of Bergen, Allegaten 41, 5007, Bergen, Norway
[g] Department of Geological Sciences, University of Alabama, Tuscaloosa, AL 35487, USA
* Corresponding author: lmejia@marum.de

This PDF includes:

Supplementary Notes S1 to S4
Supplementary Figures S1 to S8
Supplementary Tables S1 to S5
Supplementary References

Other supporting material for this manuscript

Dataset S1

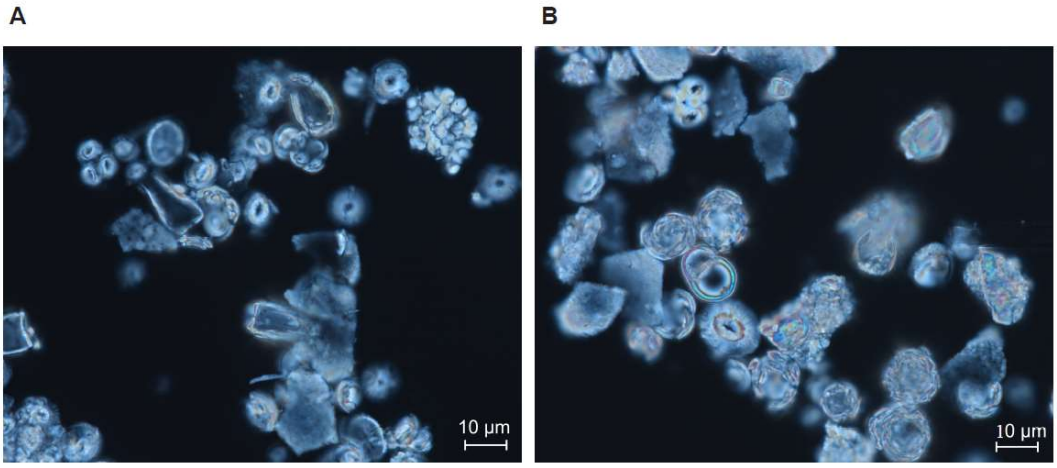

Fig. S1. Example of light microscope image of the 10-11 µm size fractions. **(A)** 4.17 Ma. **(B)** 5.79 Ma. This fraction is enriched in large non-coccolith fragments like foraminifera fragments.

Note S1. Negligible cold bias effect of *Coccolithus pelagicus* in coccolith Δ_{47} temperatures

In addition to reticulofenestrids, other species in the assemblages include *C. pelagicus*, *Calcidiscus* sp., *Helicosphaera* sp., *Sphenolithus* sp., *Discoaster* sp., and *Postosphaera* sp. (Fig. S2). Sediment trap studies from the nearby North Atlantic Bloom Experiment 48 (NABE) have shown that increased abundances of *C. pelagicus* are not observed when all other coccolithophore species have a blooming peak during spring (1). *C. pelagicus* is a dominant species in subpolar North Atlantic waters with an optimum temperature range of 2-12 °C (2, 3) and its increased abundance has been related to the presence of cyclonic eddies in the area, most likely transporting them from higher to lower latitudes (1, 4). Therefore, they are unlikely to represent a large part of the *in situ* coccolithophore production in our ODP Site 982. The presence of subpolar eddies in the area has been suggested to lead to cold biases in alkenone temperatures (4, 5). Therefore, the increased relative abundance of *C. pelagicus* in our samples at ~2, 4.2 and 14 Ma (4.2, 3.4, and 10.6%, respectively) could potentially result in a cold bias in our clumped isotope temperatures as well, possibly related to a more frequent influence of subpolar eddies.

From these three samples, however, only at ~14 Ma are clumped isotope temperatures for the large size fraction (8-10 µm; 11.02 ± 3.9 °C, 95% CI) significantly colder than for the average of other size fractions (3-5 and 5-8 µm; 21.58 ± 3.33 °C, 95% CI), and is the relative abundance of *C. pelagicus* high enough to produce a cold bias. Applying simple mass balance, and assuming all coccoliths in the 8-10 µm size fraction are *C. pelagicus* advected from colder latitudes (which is not the case), the temperature underestimation of this sample would remain 1.1 °C, which is smaller than the analytical error of clumped isotope measurements. Therefore, we can conclude that the presence of *C. pelagicus* cannot explain the observed temperature differences between alkenone and clumped isotope temperatures.

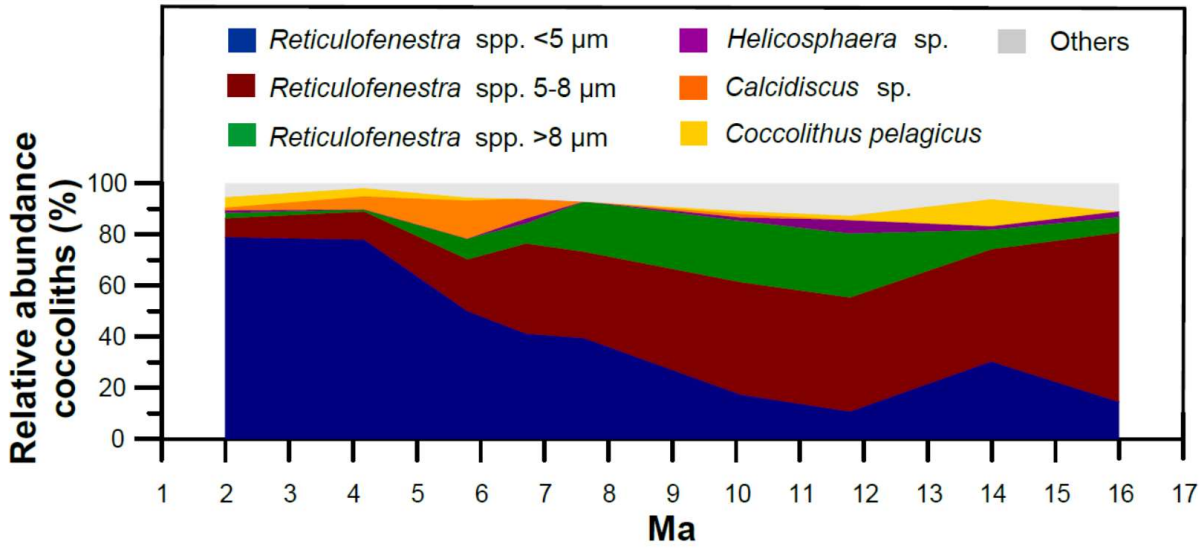

Fig. S2. Relative coccolith abundances (%) in the assemblages of sediments from ODP Site 982. Coccolith counting was estimated from the 2-10 µm. Dominant coccolithophore species are *Reticulofenestra* spp. <5 µm, *Reticulofenestra* spp. 5-8 µm, *Reticulofenestra* spp. >8 µm, *Helicosphaera* sp., *Calcidiscus* sp., and *Coccolithus pelagicus*. Other species include *Sphenolithus* sp., *Discoaster* sp., and *Postosphaera* sp., and are grouped together with the unidentifiable >2 µm carbonate fragments as "others".

Note S2. Negligible cold biases in coccolith Δ_{47} temperatures from diagenetic processes

Clumped isotope thermometry is sensitive to the presence of diagenetically-altered carbonate (6). In the case of coccolith calcite, carbonate overgrowth at the seafloor occur at colder temperatures than primary biological calcification in the euphotic ocean. Therefore, diagenesis can potentially bias reconstructed temperatures towards colder values. For our high latitude ODP 982 Site, where the temperature gradient with water depth is smaller compared to warm and more stratified waters in the tropics, diagenetic alteration is expected have a lower impact in Δ_{47} reconstructed temperatures.

SEM shows the generally good coccolith preservation in all samples (Fig. S3). Yet, regardless of the burial time, there is some carbonate overgrowth partially or completely covering the central area (Fig. S4), but in coccoliths of all ages, the rims are well defined. Overall, authigenic carbonate comprises a low proportion of analyzed carbonate. Our upper estimate of authigenic carbonate is always < 8.1% (5.8 Ma sample) and in some cases as low as 2.8% (11.8 Ma sample) (Table S1).

To understand the potential effect of post-burial alteration on Δ_{47} temperatures, we applied the diagenesis model of Stolper et al. (7) to ODP Site 982. This model estimates quantitatively the effect of diagenesis on Δ_{47} temperatures. To apply the model, we used the recrystallization rates estimated by Schrag et al. (8) for bulk carbonates in the equatorial ODP Site 807, bottom water temperatures from Lear et al. (9), average sedimentation rates of our ODP Site 982 core (36.1 meters per million years), a geothermal gradient of 30 °C per km of sediment buried, and for initial temperatures (before alteration), the alkenone derived SSTs. The results indicate larger cold offsets in older samples, with a trend of increasing diagenetic alteration (%) over time (Fig. S5A). The oldest sample (16 Ma) show up to 55% diagenetic alteration, and the youngest sample (2 Ma) > 10%. These amounts are much larger than the upper estimates of authigenic carbonate in our samples, and they are the direct result of using recrystallization rates for bulk carbonates rather than for coccolith calcite. Since coccoliths are covered

with a protective polysaccharide organic matrix which makes them resistant to carbonate alteration (10), it is expected that the high recrystallization rates observed by Schrag et al. (8) result mainly from non-coccolith carbonate. Thus, the model overestimates the effects of authigenic contributions in our samples since recrystallization rates specific to the pure coccolith fractions are expected to be significantly lower.

Although actual coccolith recrystallization rates are unknown, the model can be adjusted with lower recrystallization rates, thus allowing it to predict diagenetic alteration consistent with our overgrowth observations (e.g., < 8.1%). This was done using fractional amounts of the bulk carbonate recrystallization rates from 0.1 to 0.25 times (in increments of 0.01). Results show that the cold bias expected for the amounts of authigenic carbonate we observe is always < 2°C (Fig. S5B). Finally, as a third way to estimate the potential alteration effect, we calculate it using a simple mass balance model. We use the alkenone SST as initial temperature and deep-water temperatures (diagenesis temperature) as endmembers, and the maximum amount of overgrowth that we observe as the fraction of diagenetic calcite in each sample (f=0.081). The results are very similar to the results of the modified diagenesis model; expected offsets in Δ_{47} temperatures relative to the alkenone data are ~2°C (Fig. S5C).

Although some dissolution was observed in coccoliths of all samples, particularly in the smallest and thinnest, to date, there is no evidence that dissolution can affect clumped isotope-derived temperatures. Moreover, compared to other marine organisms like foraminifera, whose calcite is composed by several nanometer-sized crystals (11), a coccolith is a single calcite crystal characterized by its homogeneous chemistry composition (e.g. ref. (12)). In addition to being restricted to the relatively thermally-stable photic zone and not showing vertical migration behavior like foraminifera, coccolithophores can produce single coccoliths intracellularly within one hour (13), highly restricting the possibility of clumped isotopes of a single coccolith to register different temperatures during its formation. Therefore, it is highly unlikely that removal of calcite from etching can affect clumped isotope-derived temperatures from coccoliths.

Smaller size fractions, especially the fragmented ones (like the <2 µm) are expected to be more prone to diagenetic alteration compared to whole coccoliths. This is not only because the surface area to volume is higher and therefore there is more surface of interaction with water, but also because the protective polysaccharides (10, 14) may have been removed from coccolith fragments. The lack of this organic protective cover could also increase the probability of diagenetic processes affecting fragments compared to whole coccoliths. Therefore, we would expect size fractions containing important amounts of <2 µm fragments (i.e. <11 µm size fraction) to be more affected by diagenesis. However, the similar clumped isotope-derived temperatures of the <11 µm size fractions and the pure coccolith (2-10 µm) size fractions (Fig 2), which are <2 µm free, suggest that at Site 982 most of the <2 µm fragments are composed of relatively well-preserved coccolith fragments. Moreover, the Sr/Ca ratios of the <2 µm fractions (1.40-1.88 mmol/mol) are typical for coccoliths found in cultures, sediment traps and sediment cores (15), are similar to those shown by pure coccolith size fractions in this study (2-10 µm: 1.69-2.02 mmol/mol), and are higher than expected for abiogenic calcite precipitated from seawater or pore fluids (16) (Table S2). This suggests that the Mg and Al enrichment shown by trace element analysis in the <2 µm fraction is not mainly driven by diagenetic processes, but rather by an enrichment of clay. The presence of clay minerals around small coccolith fragments could have contributed to a better preservation of this size fraction.

The very low authigenic carbonate from our samples shows that the removal of <2 µm fragments from the pure coccolith 2-10 µm size fraction would have not been necessary. However, the removal of this diagenetically susceptible fraction may be required in other sediments where this fraction is altered, even if its removal increases separation time in at least ten times. This applies to old sediments, in which diagenesis is expected to have had more time to affect pristine carbonate, but also to recent ones in locations where detrital sediments in the small size fraction are important (17). Since in tropical, warm, stratified locations and time intervals temperature differences between surface and bottom waters are larger than in high latitudes like ODP Site 982, a special evaluation of the diagenetic component of these sediments is required to ensure accurate temperature reconstructions using coccolith clumped isotopes.

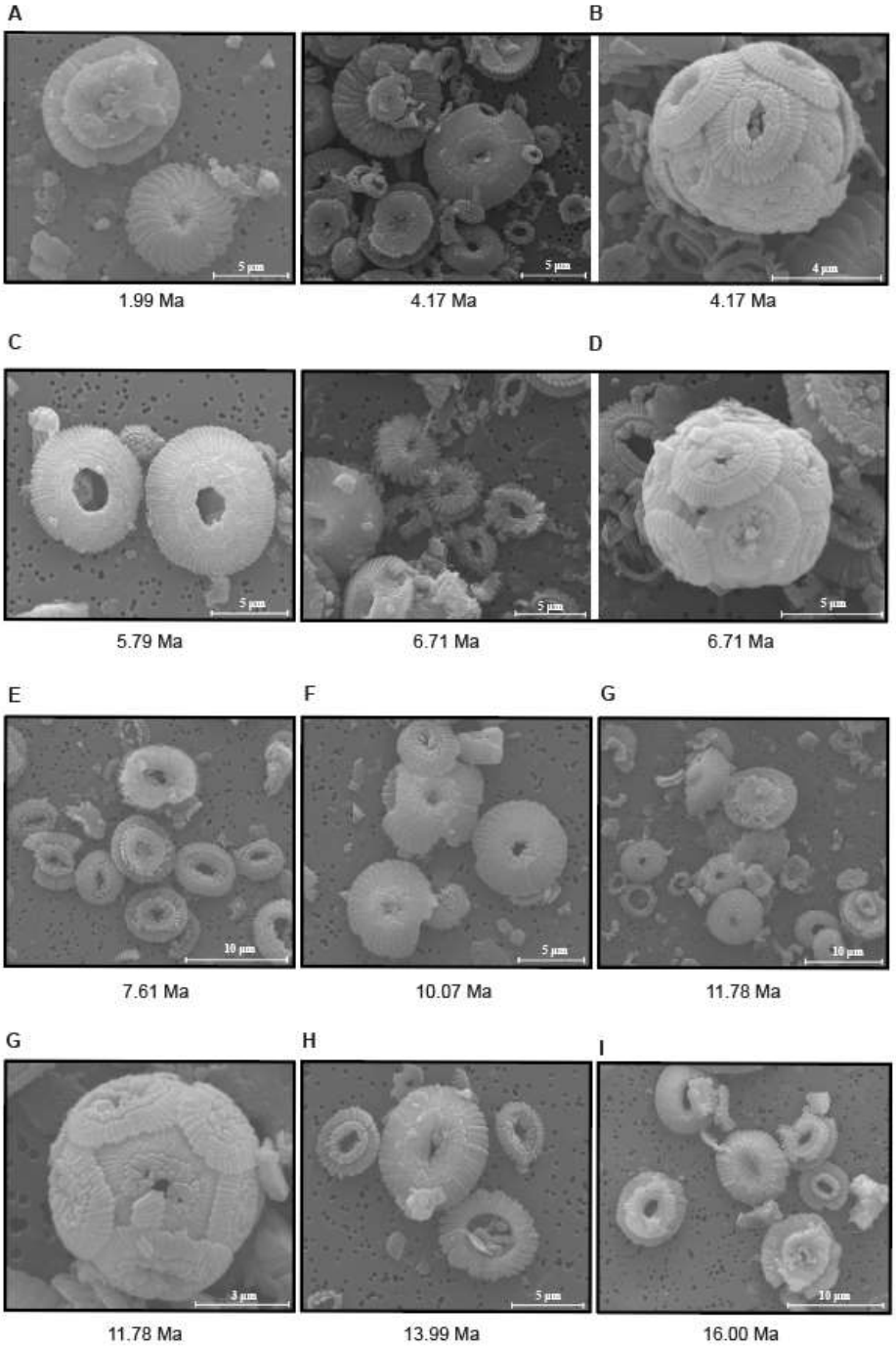

Fig. S3. Scanning Electron Microscope images of < 11 µm coccolith fractions from ODP Site 982. **(A)** 1.99 Ma. **(B)** 4.17 Ma. **(C)** 5.79 Ma. **(D)** 6.71 Ma. **(E)** 7.61 Ma. **(F)** 10.07 Ma. **(G)** 11.78 Ma. **(H)** 13.99 Ma **(I)** 16 Ma. Note that the < 11 µm size fraction contains the <2 µm and therefore some small carbonate and clay fragments are deposited on top of coccoliths and coccospheres.

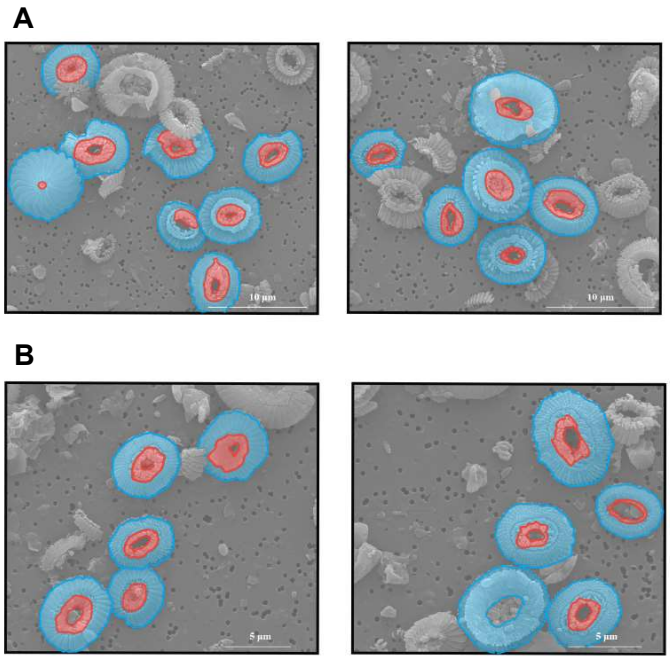

Fig. S4. Example of scanning Electron Microscope images of <11 µm coccolith fractions used for estimating coccolith surface area affected by diagenesis. (A) 7.61 Ma. **(B)** 10.07 Ma. Areas shaded in blue and red denote areas with well preserved and affected calcite, respectively. Note that the < 11 µm size fraction contains the <2 µm and therefore some small carbonate and clay fragments are deposited on top of coccoliths, but may not be authigenic calcite.

Table S1. Pristine and diagenetically altered carbonate in samples. Area of pristine and diagenetically altered carbonate (%) from SEM imaging, and amount of pristine and diagenetically altered carbonate (%), calculated following the geometrically-calculated coccolith volume plots of Young and Ziveri (18), and assuming that maximum half of the calculated volume was affected by diagenesis.

Age (Ma)	% area SEM images		% calcite in samples	
	Pristine coccolith	Authigenic calcite	Pristine coccolith	Authigenic calcite
1.99	83.9	16.1	93.1	6.9
4.17	89.0	11.0	96.5	3.5
5.79	82.1	17.9	91.9	8.1
6.71	88.5	11.5	95.9	4.1
7.61	85.9	14.1	94.3	5.7
10.07	89.2	10.8	96.5	3.5
11.78	90.4	9.6	97.2	2.8
13.99	83.8	16.2	93.1	6.9
16	85.7	14.3	94.3	5.7

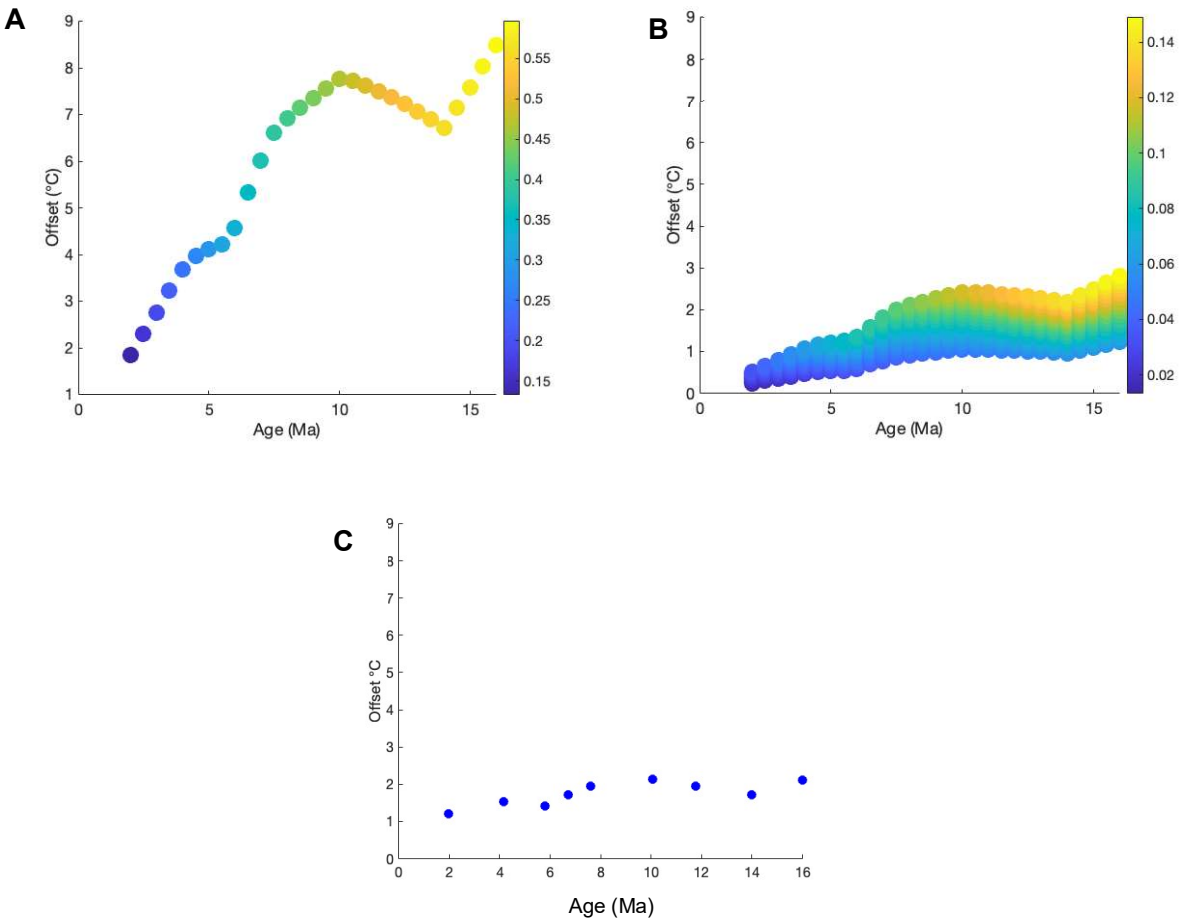

Fig. S5. **Effect of recrystallization on coccolith clumped isotope temperatures.** A) Offsets between alkenone SSTs and coccolith Δ_{47} temperatures estimated with the diagenesis model of Stolper et al. (7) and the recrystallization rates of Schrag et al. (8) for bulk carbonate. B) Offsets between alkenone SSTs and coccolith Δ_{47} temperatures estimated with the diagenesis model of Stolper et al. (7) and with fractional amounts (10-25%) of the recrystallization rates of Schrag et al. (8) for bulk carbonate. C) Offsets between alkenone SSTs and coccolith Δ_{47} temperatures estimated with a mass balance model. Colorbar in A and B is fraction carbonate recrystallized.

Table S2. Trace element analysis of the < 2 and the 2-10 µm size fractions from ODP Site 982.

Age (Ma)	Size fraction (µm)	Sr/Ca (mmol/mol)	Mg/Ca (mmol/mol)	Al/Ca (mmol/mol)
1.99	<2	1.84	4.54	3.01
4.17		1.46	11.35	2.83
5.79		1.40	5.69	1.70
6.71		1.57	4.84	1.97
7.61		1.61	8.30	3.50
10.07		1.54	5.75	1.35
11.78		1.55	4.49	1.46
13.99		1.53	3.11	0.90
16.00		1.88	4.03	1.44
1.99	2-10	2.01	2.44	0.67
4.17		2.02	2.10	0.07
5.79		1.74	1.97	0.12
6.71		1.76	1.18	0.11
7.61		1.78	1.14	0.17
10.07		1.69	1.96	0.28
11.78		1.79	1.95	0.03
13.99		1.79	1.70	0.17
16.00		1.90	1.51	0.34

Note S3. Differences in calibration approaches: "Depth of production effect"

For the North Atlantic, significantly high depth-integrated phytoplankton biomasses and chlorophyll inventories have been observed using floats (19) and by satellite and modelling studies during the cold period of mixed layer deepening (December-February) (20). A deeper production could contribute to temperature differences between coccolith clumped isotope and alkenone proxies. This "depth of production effect" is expected to be larger in lower latitudes like in the oligotrophic South Pacific and North Pacific gyres, where peak production at depth (150-200 (21) and 75-100 m (22), respectively) has been described. The same is valid for warmer intervals, as more stratified waters are expected to increase this "depth of production effect", wherewith differences between absolute reconstructions using widely-used alkenone calibrations (23, 24) (SSTs) vs. coccolith clumped isotopes (temperatures at depth of production) are also expected to be larger.

To estimate the magnitude of the "depth of production effect" for the modern North Atlantic, we calculated the differences of World Ocean Atlas (WOA) 2018 (25) average monthly temperatures between surface waters and those at 40 and 100 m for months when integrated depth and surface primary production is expected to be significant (i.e. ~from December to May/June (20); Table S3). Depths between 40 and 100 m were chosen, as 1984 cruise data for our study site from April, which is one of the months with both the highest "surface" phytoplankton biomass and coccolithophore fluxes (1, 19, 20) show significantly larger chlorophyll values between 40 and 100 m, with a peak at 60 m (26). A maximum temperature difference between surface and deeper waters of 1.6 °C was observed for June, assuming peak of production at 100 m, with decreasing magnitudes for earlier months, when the mixed layer is deeper.

Table S3. Average monthly temperatures from WOA between 1955 and 2012 for the surface ocean (0 m), at 40 and 100 m depth, for the location of ODP Site 982. Average temperatures at the same depths for the winter-spring production season (20), and differences of average monthly temperatures between surface (0 m) and 40 m and surface and 100 m depth, also shown. These differences show that for months when integrated depth and surface primary production is expected to be significant (~from December to May/June; shown in italics), alkenone temperatures calculated using SST could be up to 1.6 °C (italics, bold) higher than deeper temperatures at which alkenones may be actually produced.

	Temp. (°C); 0 m	Temp. (°C); 40 m	Temp. (°C); 100 m	Temp. diff. (°C); 0-40 m	Temp. diff. (°C); 0-100 m
Jan	*9.44*	*9.40*	*9.37*	*0.04*	*0.07*
Feb	*9.03*	*9.04*	*8.99*	*-0.01*	*0.04*
Mar	*8.95*	*8.89*	*8.91*	*0.06*	*0.04*
Apr	*9.21*	*9.02*	*8.93*	*0.19*	*0.28*
May	*9.96*	*9.52*	*9.18*	*0.44*	*0.78*
Jun	*10.84*	*10.16*	*9.24*	*0.68*	***1.60***
Jul	12.47	10.95	9.34	1.52	3.13
Aug	13.20	11.69	9.51	1.51	3.69
Sep	12.51	12.06	9.75	0.45	2.76
Oct	11.47	11.33	10.09	0.14	1.38
Nov	10.20	10.11	10.00	0.09	0.20
Dec	*9.51*	*9.49*	*9.45*	*0.02*	*0.06*
Av. winter-spring	*9.60*	*9.40*	*9.20*	0.22	*0.45*

Note S4. Differences in calibration approaches: "Season of production effect"

In places where alkenone production is seasonal, like in the North Atlantic, coretop calibrations using annual (23) or warm season (24) SSTs, may introduce seasonal biases in $U^{k'}_{37}$ temperatures (27). Therefore, the ideal calibration should use temperatures of periods when most of the alkenones that are preserved in the sediment are produced. We calculated the temperature differences potentially caused by this "season of production effect". For this, we compared WOA average monthly SSTs between the months used by alkenone calibrations (all year (23), August-October (24)) and those of months reported to coincide with maximum surface production in the North Atlantic (1, 4, 19, 20, 28), or significant depth-integrated primary production (20) (winter-spring; Table S4). Flux peaks in sediment traps may lag maximum surface chlorophyll by 1-2 months due to long settling times (29). The maximum coccolith export in March-May recorded by the 1 km trap at the nearby NABE-48 site (1) and the slightly later alkenone flux peak in the deeper 3.7 km trap (April-June (4)) are also consistent with winter-spring production (20). This simple analysis shows that the application of the Bayspline calibration (24), which uses significantly warmer temperatures than those of actual alkenone production, can lead to up to 3°C overestimates in alkenone-calculated temperatures. Smaller overestimates are estimated when the core top calibration (23) is used (up to 1.2 °C).

Table S4. Average monthly SSTs from WOA between 1955 and 2012 for the location of ODP Site 982 in the North Atlantic. This includes average monthly SSTs used for the alkenone Bayspline (24) and the core top (23) calibrations; average monthly SSTs of periods of surface coccolith peak export (1), alkenone peak export (4), and phytoplankton surface blooms (19, 20, 28) in the North Atlantic, and average monthly SSTs of periods of significant depth-integrated and surface phytoplankton production in the North Atlantic (20). Temperature differences between average monthly SSTs of considered periods for alkenone calibrations and actual production periods, show that the maximum "season of production effect" can reach up to 3.0 °C when comparing the Bayspline calibration and the Broerse et al. (1) dataset (bold, italics).

		Surface							Depth-integrated + surface
WOA average monthly SST (°C)		**Bayspline** (24)	**Core top** (23)	**Filippova et al.** (28)	**Mignot et al.** (19)	**Broerse et al.** (1)	**Rosell-Melè et al.** (4)	**Behrenfeld et al.** (20)	**Behrenfeld et al.** (20)
		Aug-Oct	**Mean annual**	**Mar-Aug**	**Apr-May**	**Mar-May**	**Apr-Aug**	**Apr-Jul**	**Dec-Jun**
Jan	**9.44**								
Feb	**9.03**								
Mar	**8.95**								9.6
Apr	**9.21**				9.6	9.4			
May	**9.96**			10.8				10.6	
Jun	**10.84**		10.6				11.1		
Jul	**12.47**								
Aug	**13.20**								
Sep	**12.51**	12.4							
Oct	**11.47**								
Nov	**10.20**								
Dec	**9.51**								
Difference to Bayspline				1.6	2.8	***3.0***	1.3	1.8	2.8
Difference to core top				-0.2	1.0	1.2	-0.6	-0.1	1.0

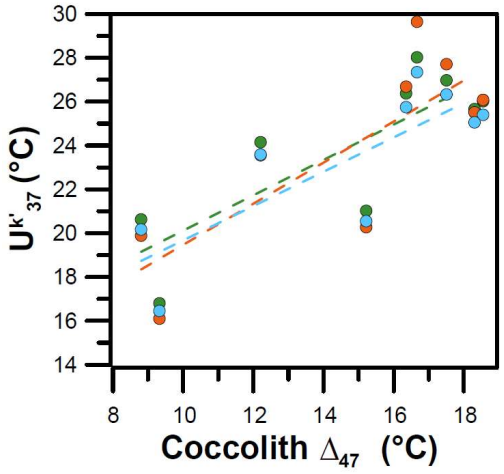

Figure S6. Alkenone SSTs as a function of coccolith clumped isotope temperatures from ODP Site 982 samples. Positive correlations between proxies are significant and are calculated using temperatures from the 2-10 µm coccolith size fractions. Correlations obtained using the *E. huxleyi* 55a batch culture (31) (r = 0.82, p = 0.007), the core top (23) (r = 0.82, p = 0.007) and the Bayspline (24) (r = 0.80, p = 0.009) calibrations shown in light blue, green and orange, respectively.

Table S5. Maximum and minimum temperatures derived from applying eleven different *Emiliania huxleyi* and *Gephyrocapsa oceanica* batch culture calibrations (30) **to our ODP Site 982 $U^{k'}_{37}$ measurements.** This includes the widely used *E. huxleyi* 55a batch culture calibration of Prahl et al. (31). Temperature differences between culture calibrations can reach up to 8 °C for a given $U^{k'}_{37}$ value (bold, italics). Alkenone temperatures obtained using the Bayspline (24) and the core top (23) calibrations, and coccolith clumped isotope temperatures are shown for comparison.

Age (Ma)	$U^{k'}_{37}$	$U^{k'}_{37}$ culture calibr. (30, 31) (°C)		Max-Min culture calibr. (30, 31) (°C)	Bayspline (24) $U^{k'}_{37}$ (°C)	Core top (23) $U^{k'}_{37}$ (°C)	Coccolith Δ_{47} (°C)
		Max	Min				
1.99	0.5984	23.8	16.5	7.4	16.1	16.8	9.3
4.17	0.7377	27.7	20.5	7.2	20.3	21.0	15.2
5.79	0.7247	27.4	20.2	7.2	19.9	20.6	8.8
6.71	0.8410	30.6	23.4	7.2	23.6	24.2	12.2
7.61	0.9026	32.3	24.9	7.4	26.1	26.0	18.5
10.07	0.9342	33.2	25.5	7.7	27.7	27.0	17.5
11.78	0.9145	32.7	25.2	7.5	26.7	26.4	16.4
13.99	0.8908	32.0	24.7	7.4	25.5	25.7	18.3
16.00	0.9687	34.2	26.2	***8.0***	29.6	28.0	16.7

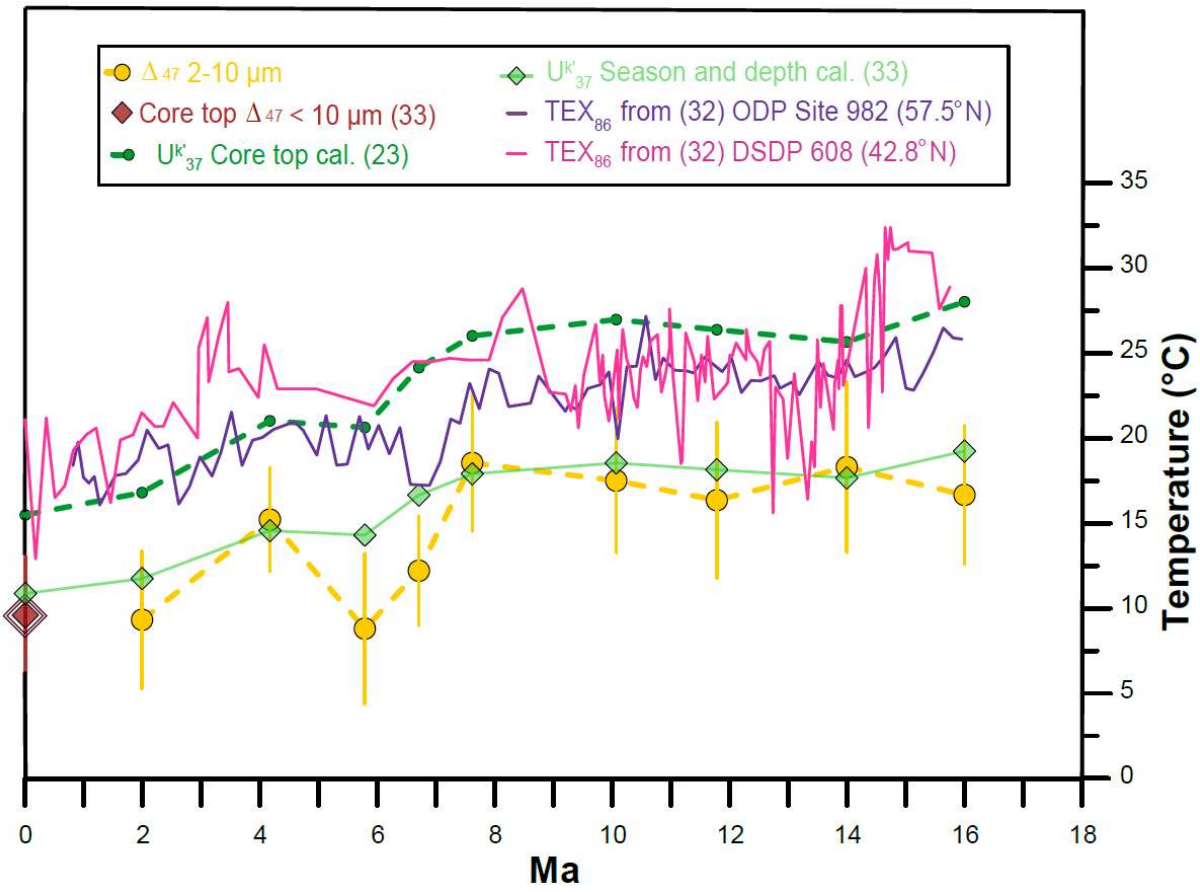

Figure S7. Coccolith clumped isotope, alkenone, and TEX_{86} temperature evolution in ODP Site 982 and DSDP Site 608 (subtropical gyre). TEX_{86} temperatures from DSDP Site 608 (pink line) and from ODP Site 982 (purple line) from the study of Super et al. (32), showing similar absolute values despite the 14.7° difference in latitudes. We include temperatures from ODP Site 982 (this study) derived from alkenones applying the core top ((23); green) and a calibration that considers the season and depth of production ((33); light green diamonds), and coccolith Δ_{47} calcification temperatures (2-11 µm: yellow). TEX_{86} temperatures were calculated using the BAYSPAR (34) calibration. Coretop alkenone and coccolith Δ_{47} temperatures from the study of Mejía et al. (33) in our same Site are also included. Error bars in coccolith Δ_{47} calcification temperatures record denote the 95% CI.

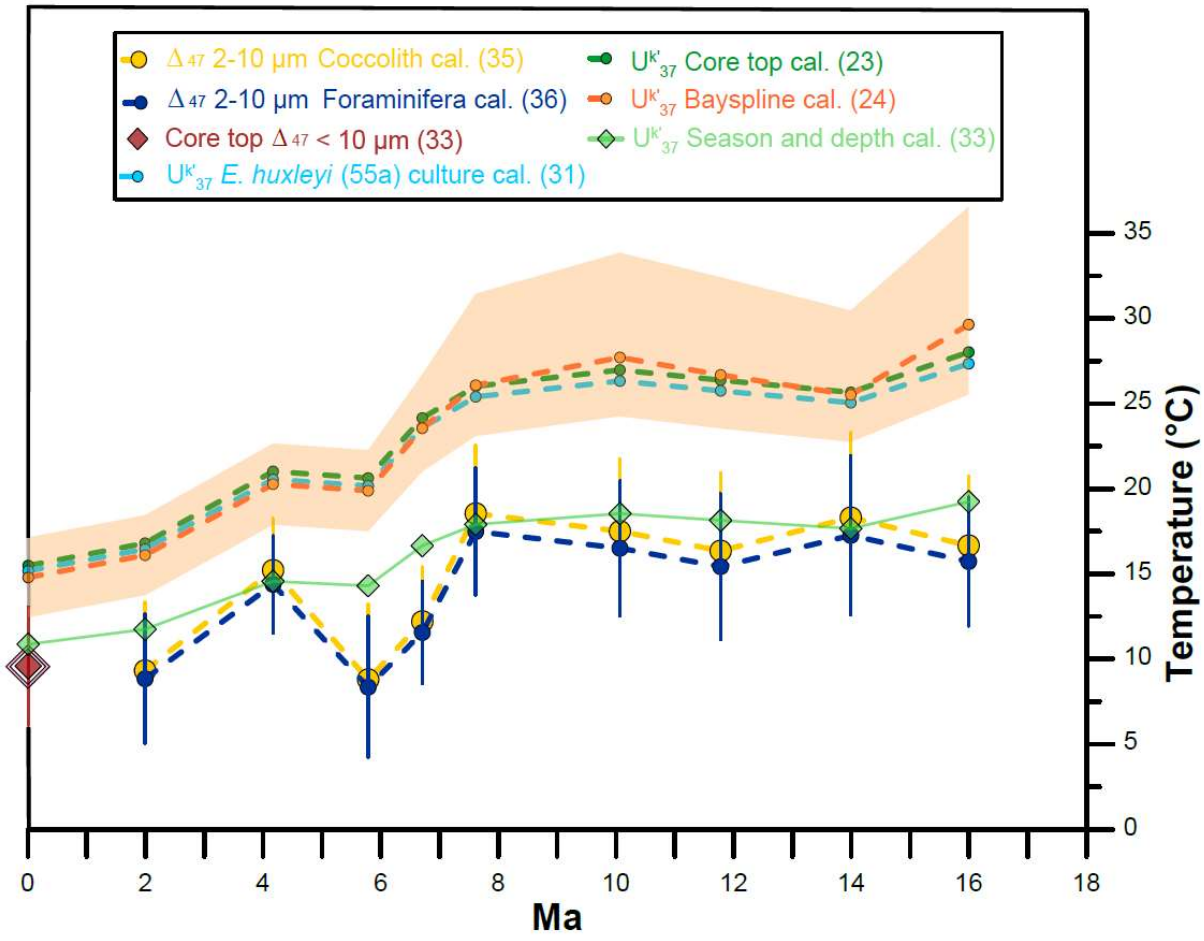

311

312 **Figure S8. Coccolith clumped isotope temperature records obtained using different biogenic Δ_{47}**
313 **calibrations, and alkenone temperature evolution in ODP Site 982.** Δ_{47} calcification temperatures
314 from the pure coccolith 2-10 µm size fraction derived by applying the culture coccolith calibration ((35);
315 yellow), and the foraminifera calibration ((36); dark blue), showing the remarkable similarities between
316 both records. Alkenone temperatures from the same samples calculated using the core top ((23); green),
317 Bayspline ((24); orange), *E. huxleyi* 55a batch culture ((31); light blue), and a calibration that considers
318 the season and depth of production ((33); light green diamonds). Coretop alkenone and coccolith Δ_{47}
319 temperatures from the study of Mejía et al. (33) in our same site are also included. Orange shaded area
320 represents the 95% CI according to the Bayspline calibration. Error bars in coccolith Δ_{47} calcification
321 temperatures record denote the 95% CI.
322

323 **References**
324

325 1. A. T. C. Broerse, P. Ziveri, J. E. Van Hinte, S. Honjo, Coccolithophore export production, species
326 composition, and coccolith-CaCO3 fluxes in the NE Atlantic (34 °N 21 °W and 48 °N 21 °W). *Deep*
327 *Sea Res 2 Top Stud Oceanogr* **47**, 1877–1905 (2000).

328 2. A. McIntyre, A. W. H. Bé, Modern coccolithophoridae of the atlantic ocean-I. Placoliths and
329 cyrtoliths. *Deep-Sea Research and Oceanographic Abstracts* **14**, 561–597 (1967).

3. H. Okada, A. McIntyre, Seasonal distribution of modern coccolithophores in the western North Atlantic Ocean. *Mar Biol* **54**, 319–328 (1979).

4. A. Rosell-Melé, P. Comes, P. J. Müller, P. Ziveri, Alkenone fluxes and anomalous UK'37 values during 1989-1990 in the Northeast Atlantic (48°N 21°W). *Mar Chem* **71**, 251–264 (2000).

5. A. Auderset, *et al.*, Gulf Stream intensification after the early Pliocene shoaling of the Central American Seaway. *Earth Planet Sci Lett* **520**, 268–278 (2019).

6. J. M. Eiler, "Clumped-isotope" geochemistry-The study of naturally-occurring, multiply-substituted isotopologues. *Earth Planet Sci Lett* **262**, 309–327 (2007).

7. D. A. Stolper, J. M. Eiler, J. A. Higgins, Modeling the effects of diagenesis on carbonate clumped-isotope values in deep- and shallow-water settings. *Geochim Cosmochim Acta* **227**, 264–291 (2018).

8. D. P. Schrag, D. J. DePaolo, F. M. Richter, Reconstructing past sea surface temperatures: Correcting for diagenesis of bulk marine carbonate. *Geochim Cosmochim Acta* **59**, 2265–2278 (1995).

9. C. H. Lear, H. Elderfield, P. A. Wilson, Cenozoic deep-sea temperatures and global ice volumes from Mg/Ca in benthic foraminiferal calcite. *Science (1979)* **287**, 269–272 (2000).

10. T. Hassenkam, A. Johnsson, K. Bechgaard, S. L. S. Stipp, Tracking single coccolith dissolution with picogram resolution and implications for CO2 sequestration and ocean acidification. *Proc Natl Acad Sci U S A* **108**, 8571–8576 (2011).

11. D. E. Jacob, R. Wirth, O. B. A. Agbaje, O. Branson, S. M. Eggins, Planktic foraminifera form their shells via metastable carbonate phases. *Nat Commun* **8**, 1–9 (2017).

12. H. Stoll, *et al.*, Insights on coccolith chemistry from a new ion probe method for analysis of individually picked coccoliths. *Geochemistry, Geophysics, Geosystems* **8**, Q06020 (2007).

13. L. M. Mejía, *et al.*, Controls over $\delta^{44/40}$Ca and Sr/Ca variations in coccoliths: New perspectives from laboratory cultures and cellular models. *Earth Planet Sci Lett* **481** (2018).

14. T.-C. Chiu, W. S. Broecker, Toward better paleocarbonate ion reconstructions: New insights regarding the CaCO3 size index. *Paleoceanography* **23**, PA2216 (2008).

15. L. M. Mejía, *et al.*, Effects of midlatitude westerlies on the paleoproductivity at the Agulhas Bank slope during the penultimate glacial cycle: Evidence from coccolith Sr/Ca ratios. *Paleoceanography* **29** (2014).

16. F. M. Richter, Y. Liang, The rate and consequences of Sr diagenesis in deep-sea carbonates. *Earth Planet Sci Lett* **117**, 553–565 (1993).

17. D. A. Hodell, *et al.*, Anatomy of Heinrich Layer 1 and its role in the last deglaciation. *Paleoceanography* **32**, 284–303 (2017).

18. J. R. Young, P. Ziveri, Calculation of coccolith volume and its use in calibration of carbonate flux estimates. *Deep Sea Res 2 Top Stud Oceanogr* **47**, 1679–1700 (2000).

19. A. Mignot, R. Ferrari, H. Claustre, Floats with bio-optical sensors reveal what processes trigger the North Atlantic bloom. *Nat Commun* **9**, 1–9 (2018).

20. M. J. Behrenfeld, S. C. Doney, I. Lima, E. S. Boss, D. A. Siegel, Annual cycles of ecological disturbance and recovery underlying the subarctic Atlantic spring plankton bloom. *Global Biogeochem Cycles* **27**, 526–540 (2013).

21. L. Beaufort, M. Couapel, N. Buchet, H. Claustre, C. Goyet, Calcite production by coccolithophores in the south east Pacific Ocean. *Biogeosciences* **5**, 1101–1117 (2008).

22. M. Y. Cortés, J. Bollmann, H. R. Thierstein, Coccolithophore ecology at the HOT station ALOHA, Hawaii. *Deep Sea Res 2 Top Stud Oceanogr* **48**, 1957–1981 (2001).

23. P. J. Müller, G. Kirst, G. Ruhland, I. Von Storch, A. Rosell-Melé, Calibration of the alkenone paleotemperature index UK'37 based on core-tops from the eastern South Atlantic and the global ocean (60°N-60°S). *Geochim Cosmochim Acta* **62**, 1757–1772 (1998).

24. J. E. Tierney, M. P. Tingley, BAYSPLINE: A New Calibration for the Alkenone Paleothermometer. *Paleoceanogr Paleoclimatol* **33**, 281–301 (2018).

25. R. A. Locarnini, *et al.*, *World Ocean Atlas 2018, Volume 1: Temperature.*, A. Mishonov Technical Ed, Ed. (NOAA Atlas NESDIS 81, 2018).

26. R. Sauzède, *et al.*, Vertical distribution of chlorophyll a concentration and phytoplankton community composition from in situ fluorescence profiles: a first database for the global ocean. *Earth Syst Sci Data* **7**, 261–273 (2015).

27. A. Rosell-Melé, F. G. Prahl, Seasonality of UK'37 temperature estimates as inferred from sediment trap data. *Quat Sci Rev* **72**, 128–136 (2013).

28. A. Filippova, M. Kienast, M. Frank, R. R. Schneider, Alkenone paleothermometry in the North Atlantic: A review and synthesis of surface sediment data and calibrations. *Geochemistry, Geophysics, Geosystems* **17**, 1370–1382 (2016).

29. P. P. Newton, R. S. Lampitt, T. D. Jickells, P. King, C. Boutle, Temporal and spatial variability of biogenic particles fluxes during the JGOFS northeast Atlantic process studies at 47°N, 20°W. *Deep-Sea Research Part I* **41**, 1617–1642 (1994).

30. W. J. D'Andrea, S. Theroux, R. S. Bradley, X. Huang, Does phylogeny control U37K-temperature sensitivity Implications for lacustrine alkenone paleothermometry. *Geochim Cosmochim Acta* **175**, 168–180 (2016).

31. F. G. Prahl, L. A. Muehlhausen, D. L. Zahnle, Further evaluation of long-chain alkenones as indicators of paleoceanographic conditions. *Geochim Cosmochim Acta* **52**, 2303–2310 (1988).

32. J. R. Super, *et al.*, Miocene Evolution of North Atlantic Sea Surface Temperature. *Paleoceanogr Paleoclimatol* **35**, e2019PA003748 (2020).

33. L. M. Mejía, *et al.*, Clumped isotopes in globally distributed Holocene coccoliths reveal their habitat depth. *Earth Planet Sci Lett* **619**, 118313 (2023).

402 34. J. E. Tierney, M. P. Tingley, A TEX86 surface sediment database and extended Bayesian
403 calibration. *Scientific Data 2015 2:1* **2**, 1–10 (2015).

404 35. A. J. Clark, I. Torres-Romero, M. Jaggi, S. M. Bernasconi, H. M. Stoll, Coccolithophorids
405 precipitate carbonate in clumped isotope equilibrium with seawater. *Preprint egusphere 2023-2581*
406 (2023). https://doi.org/10.5194/egusphere-2023-2581.

407 36. N. Meinicke, M. A. Reimi, A. C. Ravelo, A. N. Meckler, Coupled Mg/Ca and Clumped Isotope
408 Measurements Indicate Lack of Substantial Mixed Layer Cooling in the Western Pacific Warm
409 Pool During the Last ~5 Million Years. *Paleoceanogr Paleoclimatol* **36**, e2020PA004115 (2021).

410